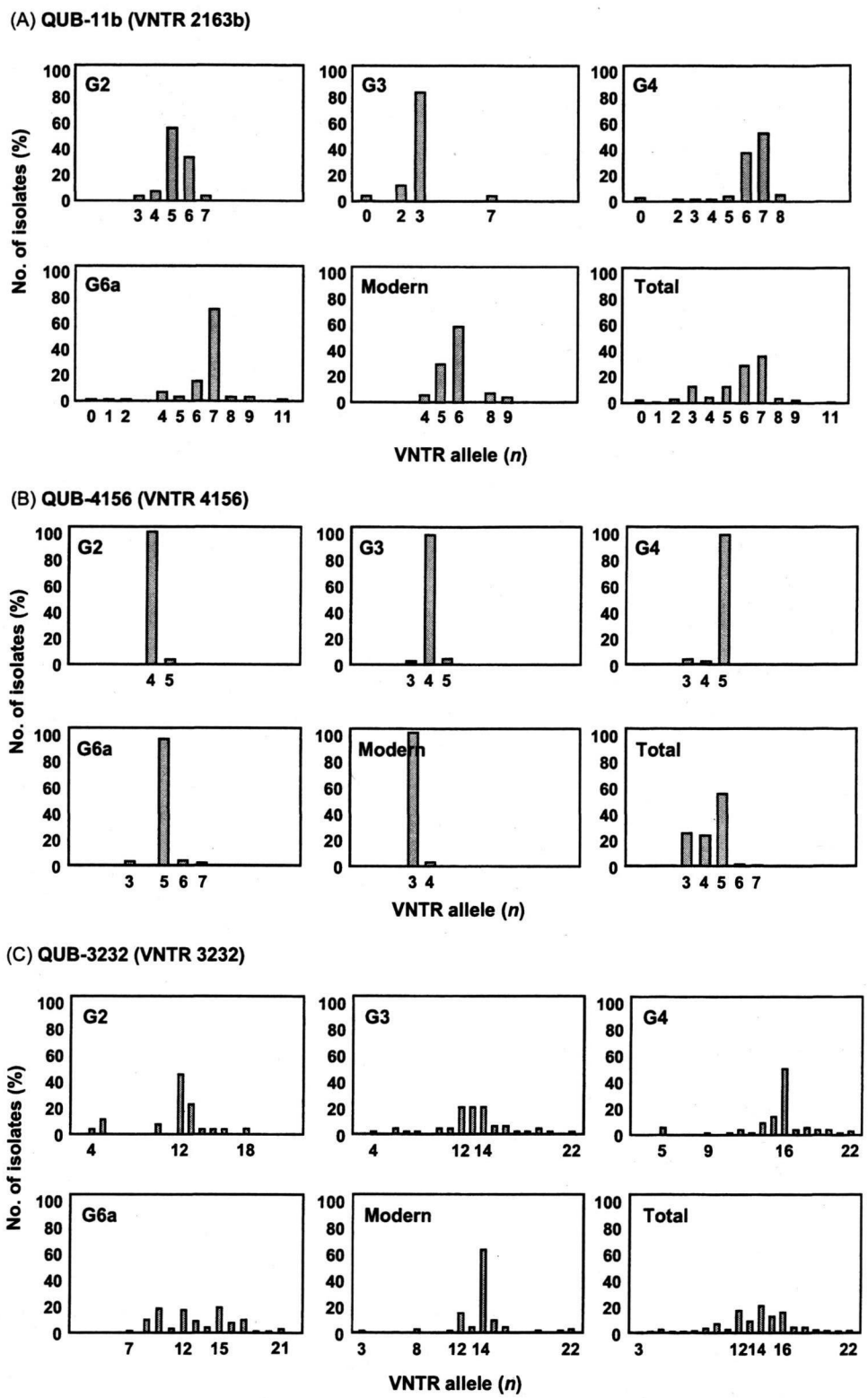

Fig. 2. Allelic distributions of three VNTR loci in the five phylogenetic groups. The *y*-axis represents the percentage of strains that possessed the given number of repetitive units (represented on the *x*-axis) in each group and total population for (A) QUB-11b, (B) QUB-4156 and (C) QUB-3232.

Beijing sublineages by VNTR analysis. An explanation of this discrepancy is that these previously identified mutations of SNPs and RD150 (Tsolaki et al., 2004; Filliol et al., 2006) may reflect a closer genetic relationship than those among ancient sublineages. Estimation of genetic diversity in each sublineage by comprehensive genomic analysis or a coalescent approach (Wirth et al., 2008) with more extensive populations requires to be conducted.

It should be noted that phylogenetic estimation with 7 VNTR loci (Table 2) cannot be applied to determine the total genetic diversity of *M. tuberculosis* owing to VNTR homoplasy. The same alleles, as listed in Table 2, were frequently identified in unrelated isolates of different lineages in many previous reports. Nevertheless, the phylogenetic interpretation by VNTR analysis was consistent with the phylogenetic characterization of the Beijing

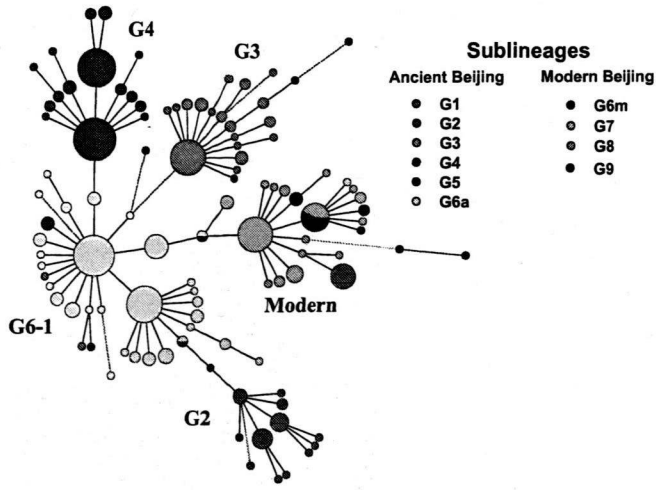

Fig. 3. A minimum spanning tree based on seven phylogenetic VNTR loci of 355 *M. tuberculosis* Beijing isolates. The 107 circles depicted correspond to the different types discriminated by these seven loci of VNTR genotypes. The designation of each circle and line in the tree is the same as in Fig. 1.

family strains isolated from Eurasia. For example, many VNTR profiles obtained from the northwest of Russia and Beijing City, China, indicated QUB-4156 = 3 and Mtub21 = 4 in the respective population analyses (Mokrousov et al., 2008; Jiao et al., 2008). Their VNTR genotypes were observed to cluster into the same branch as that in the case of modern Beijing strains from Japan in the MST construction with the 355 isolates included in this study (data not shown). This result is concordant with the fact that the modern Beijing subfamily is predominant in Eurasian countries. We also found that ancient Beijing strains belonging to ST3 from China and Mongolia exhibited an MIRU10 = 1, which was concordant with the results for the Japanese population (Wada et al., 2009). This allele was identified in other reports of VNTR analysis of the Beijing family strains not only from Japan but also other countries (Mokrousov et al., 2004; Jiao et al., 2008; Dou et al., 2008). It is important to verify such phylogenetic traits of VNTR among the Beijing family strains with different origins worldwide in order to apply VNTR genotyping for international comparison of this lineage.

Phylogenetic estimation of *M. tuberculosis* strains by VNTR genotyping enables us to discriminate between the clinical isolates accurately, although such application of VNTR genotyping is restricted to a population with low genetic diversity. Most previous reports of VNTR genotyping methods are concerned with their discrimination between strains and genotypic matching for epidemiological use. If we employ VNTR loci not only for the purpose of discrimination but also for phylogenetic estimation, VNTR genotyping will become a simple and systematic tool for molecular epidemiology and population analysis of *M. tuberculosis*.

In conclusion, we identified putative phylogenetic traces of the *M. tuberculosis* Beijing family in VNTR alleles. The phylogenetic interpretation by VNTR analysis will improve as a genotyping method and will provide clues for the microevolutionary estimation in the case of clonal populations of *M. tuberculosis*.

Acknowledgements

We thank Dr. Atsushi Hase (Osaka City Institute of Public Health and Environmental Sciences, Osaka, Japan) for his helpful supports. This work was supported by grants from the United States–Japan Cooperative Medical Science Program against Tuberculosis and Leprosy, and grants from JSPS Grant-in-Aid for Scientific Research (A) (20249007).

Appendix A. Supplementary data

Supplementary data associated with this article can be found, in the online version, at doi:10.1016/j.meegid.2009.06.012.

References

Bifani, P.J., Mathema, B., Kurepina, N.E., Kreiswirth, B.N., 2002. Global dissemination of the *Mycobacterium tuberculosis* W-Beijing family strains. Trends Microbiol. 10, 45–52.

Chiou, C.S., Watanabe, H., Wang, Y.W., Wang, W.L., Terajima, J., Thong, K.L., Phung, D.C., Tung, S.K., 2009. Utility of multilocus variable-number tandem-repeat analysis as a molecular tool for phylogenetic analysis of *Shigella sonnei*. J. Clin. Microbiol. 47, 1149–1154.

Cole, S.T., Brosch, R., Parkhill, J., Garnier, T., Churcher, C., Harris, D., Gordon, S.V., Eiglmeier, K., Gas, S., Barry 3rd, C.E., Tekaia, F., Badcock, K., Basham, D., Brown, D., Chillingworth, T., Connor, R., Davies, R., Devlin, K., Feltwell, T., Gentles, S., Hamlin, N., Holroyd, S., Hornsby, T., Jagels, K., Krogh, A., McLean, J., Moule, S., Murphy, L., Oliver, K., Osborne, J., Quail, M.A., Rajandream, M.A., Rogers, J., Rutter, S., Seeger, K., Skelton, J., Squares, R., Squares, S., Sulston, J.E., Taylor, K., Whitehead, S., Barrell, B.G., 1998. Deciphering the biology of *Mycobacterium tuberculosis* from the complete genome sequence. Nature 393, 537–544.

Dou, H.Y., Lu, J.J., Lin, C.W., Chang, J.R., Sun, J.R., Su, I.J., 2008. Molecular epidemiology and evolutionary genetics of *Mycobacterium tuberculosis* in Taipei. BMC Infect. Dis. 8, 170.

Filliol, I., Driscoll, J.R., Van Soolingen, D., Kreiswirth, B.N., Kremer, K., Valetudie, G., Anh, D.D., Barlow, R., Banerjee, D., Bifani, P.J., Brudey, K., Cataldi, A., Cooksey, R.C., Cousins, D.V., Dale, J.W., Dellagostin, O.A., Drobniewski, F., Engelmann, G., Ferdinand, S., Gascoyne-Binzi, D., Gordon, M., Gutierrez, M.C., Haas, W.H., Heersma, H., Kallenius, G., Kassa-Kelembho, E., Koivula, T., Ly, H.M., Makristathis, A., Mammina, C., Martin, G., Mostrom, P., Mokrousov, I., Narbonne, V., Narvskaya, O., Nastasi, A., Niobe-Eyangoh, S.N., Pape, J.W., Rasolofo-Razanamparany, V., Ridell, M., Rossetti, M.L., Stauffer, F., Suffys, P.N., Takiff, H., Texier-Maugein, J., Vincent, V., De Waard, J.H., Sola, C., Rastogi, N., 2002. Global distribution of *Mycobacterium tuberculosis* spoligotypes. Emerg. Infect. Dis. 8, 1347–1349.

Filliol, I., Driscoll, J.R., van Soolingen, D., Kreiswirth, B.N., Kremer, K., Valetudie, G., Dang, D.A., Barlow, R., Banerjee, D., Bifani, P.J., Brudey, K., Cataldi, A., Cooksey, R.C., Cousins, D.V., Dale, J.W., Dellagostin, O.A., Drobniewski, F., Engelmann, G., Ferdinand, S., Gascoyne-Binzi, D., Gordon, M., Gutierrez, M.C., Haas, W.H., Heersma, H., Kassa-Kelembho, E., Ho, M.L., Makristathis, A., Mammina, C., Martin, G., Mostrom, P., Mokrousov, I., Narbonne, V., Narvskaya, O., Nastasi, A., Niobe-Eyangoh, S.N., Pape, J.W., Rasolofo-Razanamparany, V., Ridell, M., Rossetti, M.L., Stauffer, F., Suffys, P.N., Takiff, H., Texier-Maugein, J., Vincent, V., de Waard, J.H., Sola, C., Rastogi, N., 2003. Snapshot of moving and expanding clones of *Mycobacterium tuberculosis* and their global distribution assessed by spoligotyping in an international study. J. Clin. Microbiol. 41, 1963–1970.

Filliol, I., Motiwala, A.S., Cavatore, M., Qi, W., Hazbon, M.H., Bobadilla del Valle, M., Fyfe, J., Garcia-Garcia, L., Rastogi, N., Sola, C., Zozio, T., Guerrero, M.I., Leon, C.I., Crabtree, J., Angiuoli, S., Eisenach, K.D., Durmaz, R., Joloba, M.L., Rendon, A., Sifuentes-Osornio, J., Ponce de Leon, A., Cave, M.D., Fleischmann, R., Whittam, T.S., Alland, D., 2006. Global phylogeny of *Mycobacterium tuberculosis* based on single nucleotide polymorphism (SNP) analysis: insights into tuberculosis evolution, phylogenetic accuracy of other DNA fingerprinting systems, and recommendations for a minimal standard SNP set. J. Bacteriol. 188, 759–772.

Gagneux, S., DeRiemer, K., Van, T., Kato-Maeda, M., de Jong, B.C., Narayanan, S., Nicol, M., Niemann, S., Kremer, K., Gutierrez, M.C., Hilty, M., Hopewell, P.C., Small, P.M., 2006. Variable host–pathogen compatibility in *Mycobacterium tuberculosis*. Proc. Natl. Acad. Sci. U.S.A. 103, 2869–2873.

Glynn, J.R., Whiteley, J., Bifani, P.J., Kremer, K., van Soolingen, D., 2002. Worldwide occurrence of Beijing/W strains of *Mycobacterium tuberculosis*: a systematic review. Emerg. Infect. Dis. 8, 843–849.

Grant, A., Arnold, C., Thorne, N., Gharbia, S., Underwood, A., 2008. Mathematical modelling of *Mycobacterium tuberculosis* VNTR loci estimates a very slow mutation rate for the repeats. J. Mol. Evol. 66, 565–574.

Gutacker, M.M., Mathema, B., Soini, H., Shashkina, E., Kreiswirth, B.N., Graviss, E.A., Musser, J.M., 2006. Single-nucleotide polymorphism-based population genetic analysis of *Mycobacterium tuberculosis* strains from 4 geographic sites. J. Infect. Dis. 193, 121–128.

Hirano, K., Kazumi, Y., Abe, C., Mori, T., Aoki, M., Aoyagi, T., 1996. Resistance to antituberculosis drugs in Japan. Tuber. Lung Dis. 77, 130–135.

Hirsh, A.E., Tsolaki, A.G., DeRiemer, K., Feldman, M.W., Small, P.M., 2004. Stable association between strains of *Mycobacterium tuberculosis* and their human host populations. Proc. Natl. Acad. Sci. U.S.A. 101, 4871–4876.

Iwamoto, T., Yoshida, S., Suzuki, K., Tomita, M., Fujiyama, R., Tanaka, N., Kawakami, Y., Ito, M., 2007. Hypervariable loci that enhance the discriminatory ability of newly proposed 15-loci and 24-loci variable-number tandem repeat typing method on *Mycobacterium tuberculosis* strains predominated by the Beijing family. FEMS Microbiol. Lett. 270, 67–74.

Iwamoto, T., Yoshida, S., Suzuki, K., Wada, T., 2008. Population structure analysis of the *Mycobacterium tuberculosis* Beijing family indicates an association between certain sublineages and multidrug resistance. Antimicrob. Agents Chemother. 52, 3805–3809.

Jiao, W.W., Mokrousov, I., Sun, G.Z., Guo, Y.J., Vyazovaya, A., Narvskaya, O., Shen, A.D., 2008. Evaluation of new variable-number tandem-repeat systems for typing *Mycobacterium tuberculosis* with Beijing genotype isolates from Beijing, China. J. Clin. Microbiol. 46, 1045–1049.

Kremer, K., Glynn, J.R., Lillebaek, T., Niemann, S., Kurepina, N.E., Kreiswirth, B.N., Bifani, P.J., van Soolingen, D., 2004. Definition of the Beijing/W lineage of *Mycobacterium tuberculosis* on the basis of genetic markers. J. Clin. Microbiol. 42, 4040–4049.

Liao, J.C., Li, C.C., Chiou, C.S., 2006. Use of a multilocus variable-number tandem repeat analysis method for molecular subtyping and phylogenetic analysis of *Neisseria meningitidis* isolates. BMC Microbiol. 6, 44.

Lindstedt, B.A., 2005. Multiple-locus variable number tandem repeats analysis for genetic fingerprinting of pathogenic bacteria. Electrophoresis 26, 2567–2582.

Maeda, S., Murase, Y., Mitarai, S., Sugawara, I., Kato, S., 2008. Rapid, simple genotyping method by the variable numbers of tandem repeats (VNTR) for *Mycobacterium tuberculosis* isolates in Japan—analytical procedure of JATA (12)-VNTR. Kekkaku 83, 673–678.

Mokrousov, I., Narvskaya, O., Otten, T., Vyazovaya, A., Limeschenko, E., Steklova, L., Vyshnevskyi, B., 2002. Phylogenetic reconstruction within *Mycobacterium tuberculosis* Beijing genotype in northwestern Russia. Res. Microbiol. 153, 629–637.

Mokrousov, I., Narvskaya, O., Limeschenko, E., Vyazovaya, A., Otten, T., Vyshnevskiy, B., 2004. Analysis of the allelic diversity of the mycobacterial interspersed repetitive units in *Mycobacterium tuberculosis* strains of the Beijing family: practical implications and evolutionary considerations. J. Clin. Microbiol. 42, 2438–2444.

Mokrousov, I., Ly, H.M., Otten, T., Lan, N.N., Vyshnevskyi, B., Hoffner, S., Narvskaya, O., 2005. Origin and primary dispersal of the *Mycobacterium tuberculosis* Beijing genotype: clues from human phylogeography. Genome Res. 15, 1357–1364.

Mokrousov, I., Jiao, W.W., Sun, G.Z., Liu, J.W., Valcheva, V., Li, M., Narvskaya, O., Shen, A.D., 2006. Evolution of drug resistance in different sublineages of *Mycobacterium tuberculosis* Beijing genotype. Antimicrob. Agents Chemother. 50, 2820–2823.

Mokrousov, I., Narvskaya, O., Vyazovaya, A., Millet, J., Otten, T., Vishnevsky, B., Rastogi, N., 2008. *Mycobacterium tuberculosis* Beijing genotype in Russia: in search of informative variable-number tandem-repeat loci. J. Clin. Microbiol. 46, 3576–3584.

Moxon, E.R., Rainey, P.B., Nowak, M.A., Lenski, R.E., 1994. Adaptive evolution of highly mutable loci in pathogenic bacteria. Curr. Biol. 4, 24–33.

Murase, Y., Mitarai, S., Sugawara, I., Kato, S., Maeda, S., 2008. Promising loci of variable numbers of tandem repeats for typing Beijing family *Mycobacterium tuberculosis*. J. Med. Microbiol. 57, 873–880.

Ohmori, M., Ishikawa, N., Yoshiyama, T., Uchimura, K., Aoki, M., Mori, T., 2002. Current epidemiological trend of tuberculosis in Japan. Int. J. Tuberc. Lung Dis. 6, 415–423.

Schouls, L.M., van der Heide, H.G., Vauterin, L., Vauterin, P., Mooi, F.R., 2004. Multiple-locus variable-number tandem repeat analysis of Dutch *Bordetella pertussis* strains reveals rapid genetic changes with clonal expansion during the late 1990s. J. Bacteriol. 186, 5496–5505.

Schouls, L.M., van der Ende, A., van de Pol, I., Schot, C., Spanjaard, L., Vauterin, P., Wilderbeek, D., Witteveen, S., 2005. Increase in genetic diversity of *Haemophilus influenzae* serotype b (Hib) strains after introduction of Hib vaccination in The Netherlands. J. Clin. Microbiol. 43, 2741–2749.

Sola, C., Filliol, I., Gutierrez, M.C., Mokrousov, I., Vincent, V., Rastogi, N., 2001. Spoligotype database of *Mycobacterium tuberculosis*: biogeographic distribution of shared types and epidemiologic and phylogenetic perspectives. Emerg. Infect. Dis. 7, 390–396.

Supply, P., Mazars, E., Lesjean, S., Vincent, V., Gicquel, B., Locht, C., 2000. Variable human minisatellite-like regions in the *Mycobacterium tuberculosis* genome. Mol. Microbiol. 36, 762–771.

Supply, P., Warren, R.M., Banuls, A.L., Lesjean, S., Van Der Spuy, G.D., Lewis, L.A., Tibayrenc, M., Van Helden, P.D., Locht, C., 2003. Linkage disequilibrium between minisatellite loci supports clonal evolution of *Mycobacterium tuberculosis* in a high tuberculosis incidence area. Mol. Microbiol. 47, 529–538.

Supply, P., Allix, C., Lesjean, S., Cardoso-Oelemann, M., Rusch-Gerdes, S., Willery, E., Savine, E., de Haas, P., van Deutekom, H., Roring, S., Bifani, P., Kurepina, N., Kreiswirth, B., Sola, C., Rastogi, N., Vatin, V., Gutierrez, M.C., Fauville, M., Niemann, S., Skuce, R., Kremer, K., Locht, C., van Soolingen, D., 2006. Proposal for standardization of optimized mycobacterial interspersed repetitive unit-variable-number tandem repeat typing of *Mycobacterium tuberculosis*. J. Clin. Microbiol. 44, 4498–4510.

Tsolaki, A.G., Hirsh, A.E., DeRiemer, K., Enciso, J.A., Wong, M.Z., Hannan, M., Goguet de la Salmoniere, Y.O., Aman, K., Kato-Maeda, M., Small, P.M., 2004. Functional and evolutionary genomics of *Mycobacterium tuberculosis*: insights from genomic deletions in 100 strains. Proc. Natl. Acad. Sci. U.S.A. 101, 4865–4870.

Tsolaki, A.G., Gagneux, S., Pym, A.S., Goguet de la Salmoniere, Y.O., Kreiswirth, B.N., Van Soolingen, D., Small, P.M., 2005. Genomic deletions classify the Beijing/W strains as a distinct genetic lineage of *Mycobacterium tuberculosis*. J. Clin. Microbiol. 43, 3185–3191.

van Belkum, A., 1999. The role of short sequence repeats in epidemiologic typing. Curr. Opin. Microbiol. 2, 306–311.

van Soolingen, D., Qian, L., de Haas, P.E., Douglas, J.T., Traore, H., Portaels, F., Qing, H.Z., Enkhsaikan, D., Nymadawa, P., van Embden, J.D., 1995. Predominance of a single genotype of *Mycobacterium tuberculosis* in countries of east Asia. J. Clin. Microbiol. 33, 3234–3238.

Wada, T., Maeda, S., Hase, A., Kobayashi, K., 2007. Evaluation of variable numbers of tandem repeat as molecular epidemiological markers of *Mycobacterium tuberculosis* in Japan. J. Med. Microbiol. 56, 1052–1057.

Wada, T., Iwamoto, T., Maeda, S., 2009. Genetic diversity of the *Mycobacterium tuberculosis* Beijing family in East Asia revealed through refined population structure analysis. FEMS Microbiol. Lett. 291, 35–43.

Wirth, T., Hildebrand, F., Allix-Beguec, C., Wolbeling, F., Kubica, T., Kremer, K., van Soolingen, D., Rusch-Gerdes, S., Locht, C., Brisse, S., Meyer, A., Supply, P., Niemann, S., 2008. Origin, spread and demography of the *Mycobacterium tuberculosis* complex. PLoS Pathog. 4, e1000160.

Jpn.J.Leprosy 78. 7-16(2009)

Temperature dependency for survival of *Mycobacterium leprae* in macrophages

Yasuo FUKUTOMI *, Yumi MAEDA, Masanori MATSUOKA, and Masahiko MAKINO

Department of Microbiology, Leprosy Research Center, National Institute of Infectious Diseases, Tokyo, Japan

[Received: 4 Aug. 2008 / Accepted: 15 Oct. 2008]

Key words : human, macrophage, mouse, *Mycobacterium leprae*, survival

Hansen's disease is caused by an infection with an intracellular pathogen, *Mycobacterium leprae*, which mainly inhabits macrophages and Schwann cells. However, little is known about the survival or growth mechanisms of the bacilli in mouse and human macrophages. In the present study, by using radiorespirometry analysis for the evaluation of the viability of *M.leprae*, we observed that *in vitro* incubation of *M.leprae*-infected macrophages at 35°C was more growth permissive than at 37°C, and supplementation with the immunosuppressive cytokine IL-10 supported the survival of the bacilli in the macrophages for 3 weeks, whereas viability of the bacilli was gradually lost if cultured without IL-10. In human macrophages, *M.leprae* retained its viability when cultured at 35°C for at least 4 weeks without IL-10. However, the viability of *M.leprae* was almost lost within 2 weeks if cultured at 37°C. These data suggest that temperature is a crucial factor for the survival of *M.leprae* in host cells.

Introduction

Hansen's disease is caused by an infection with *Mycobacterium leprae*. *M.leprae* is an intracellular pathogen, mainly residing in macrophages and Schwann cells. In patients, *M.leprae* is predominantly observed in the skin, nasal mucosa and peripheral nerves, particularly the more superficial ones. This clinical observation suggests that the optimal temperature of *M.leprae* for survival in human cells is less than 37°C [1]. In animal models, *M.leprae* multiplies in the mouse footpad where the temperature is lower than the core temperature, and the optimal temperature for the growth of *M.leprae* is reported to be in the range of several degrees above and below 30°C [2].

From another aspect, the growth of *M.leprae* seems to be largely affected by the host immune

*Corresponding author :
Department of Microbiology, Leprosy Research Center,
National Institute of Infectious Diseases
4-2-1, Aoba-cho, Higashimurayama-shi, Tokyo 189-0002, Japan
TEL : 81-42-391-8211 FAX: 81-42-394-9092
E-mail : fukutomi@nih.go.jp

response. Hansen's disease is characterized by a broad spectrum of the host immune response, such as lepromatous type (towards the increased load of bacteria) and tuberculoid type (towards the decreased bacterial load). In lepromatous type leprosy, Th-2 cytokines (IL-4, IL-5 and IL-10) are predominantly expressed in local lesions. In contrast, in tuberculoid type, Th-1 cytokines (IFN-γ, IL-2) are predominantly expressed [3]. Among cytokines, IFN-γ has been demonstrated to play a central role in activating macrophages to kill intracellular pathogens including *M.leprae*, whereas IL-10 is reported to inhibit the microbicidal activity of macrophages, resulting in the survival of the intracellular pathogen [4]. However, little is known about the survival and growth mechanisms of *M.leprae* in human macrophages since the viability of these uncultivable bacilli cannot be easily measured by in vitro study.

Previously we reported that metabolically active *M.leprae* were maintained in monolayer cultures of mouse peritoneal macrophages and supplemental IL-10 bolstered *M.leprae* metabolism in the macrophages for as long as 8 weeks. In the cell culture system temperature is extremely important and 31-33°C incubation temperature is more growth permissive than 37°C [5]. In the present study, we observed that incubation of mouse macrophages at 35°C was also more permissive than at 37°C and supplemental IL-10, but not TGF-β, supported the metabolic activity of *M.leprae* in the macrophages for several weeks. Moreover, *M.leprae* from infected human macrophages cultured in vitro sustained metabolic activity for at least 4 weeks if cultured at 35°C but not at 37°C. Collectively, these data demonstrate that temperature is one of the crucial factors for *M.leprae* survival in human host cells.

Materials and Methods

M.leprae inoculum: The Thai-53 strain of *M.leprae* [6] was maintained in continuous passage in athymic *nu/nu* mice (Clea Co, Tokyo, Japan) by inoculation of bacilli into both hind foot pads. Experiments with mice were performed in compliance with the guidelines of the Experimental Animal Committee of the National Institute of Infectious Diseases. At approximately one year post inoculation, the foot pads were processed to recover *M.leprae* by Nakamura's method with a slight modification [7]. Briefly, tissue was minced and homogenized with Hanks' balanced salt solution (HBSS) containing 0.05% Tween 80. The homogenate was centrifuged at 150×g for 10 min and supernatant of the sample homogenate was treated with 0.05% trypsin at 37°C for 60min. The suspension was centrifuged at 4,000×g for 20min and sediment was re-suspended in HBSS followed by treatment with 1% sodium hydroxide at 37°C for 15min. The treated material was washed and re-suspended in HBSS at the desired bacillary concentration. Bacillary number in each foot pad was enumerated individually according to standard techniques [8].

Cytokines: Murine recombinant IL-10 was obtained from Genzyme Corp. TGF-β was obtained from Kurashiki Bouseki (Kurashiki, Japan). Both cytokines were stored at -80°C until use.

Mouse macrophage culture: Mouse peritoneal resident cells (approximately 50% macrophages) were harvested from retired ICR mice and suspended as previously described [9] at a concentration of 2×10^6/ml in RPMI 1640 (Gibco BRL, Invitrogen Corp., Carlsbad, CA) supplemented with 15% fetal bovine serum (FBS, HyClone Laboratories, Logan UT), 25 mM N-2-

hydroxyethylpiperazine -N'- 2-ethanesulfonic acid (HEPES), 2 mM glutamine and 100μg/ml ampicillin (Sigma Chemical Co., St. Louis, MO). One half ml was seeded into 24 well tissue culture plates (Corning) containing 13 mm LUX coverslips (Nunc Thermanox coverslips, NalgeNunc, Thermo Scientific, Rochester, NY). After 20 hr adherence of the cells, macrophage monolayers were obtained after washing non-adherant cells from the coverslip with Hanks Balanced Salt Solution (HBSS, Sigma) leaving approximately 1×10^6 macrophages adhered per coverslip.

Human macrophage culture: Human peripheral blood was obtained under informed consent from healthy individuals. Peripheral blood mononuclear cells (PBMC) were isolated using Ficoll-Paque Plus (GE Healthcare Life Sciences, Buckinghamshire, HP7 9NA, UK) gradient centrifugation[10]. The cells were suspended in AIM-V medium (Gibco BRL, Invitrogen Corp., Carlsbad, CA) and 1×10^6 PBMC were cultured in a well of a 24-well tissue culture plate (Falcon, Becton Dickinson Labware, Becton Dickinson and Company, Franklin Lakes) containing 13 mm LUX coverslips at 37°C in a 5%-CO_2 incubator for adherence of monocytes. After 1 hr incubation, the coverslips were washed with HBSS to remove non-adherent cells. The monocytes on the coverslips were cultured in a new 24-well plate containing RPMI1640 medium (Sigma) supplemented with 20% FBS (Whittaker Co., Walkersville, MD), 25mM HEPES, 2mM L-glutamine and 100μg/ml ampicillin in the presence of 10 ng/ml of human M-CSF (R&D Systems, Minneapolis, MN) or 40 ng/ml of GM-CSF (R&D Systems). After 7 days, the M-CSF-conditioned macrophages (M-macrophages) and the GM-CSF-conditioned macrophages (GM-macrophages) were used for infection with *M.leprae*.

Infection of macrophages with *M.leprae*: Purified mouse macrophage monolayers were infected with fresh *M.leprae* suspended in 0.5 ml medium per well. After 4 hr incubation for mouse macrophages and 20 hr incubation for human macrophages, non-phagocytosed bacilli were removed by washing and the cultures were incubated in 1.0 ml media supplemented with the appropriate cytokine in 5% CO_2 at the appropriate experimental temperatures[9]. Media were changed and cytokines were replenished at 5 days interval.

Radiorespirometry: The macrophages were lysed with 0.1 N NaOH to release the phagocytosed *M.leprae*, and the viability of the bacilli was determined by evaluating the oxidation of ^{14}C-palmitic acid to $^{14}CO_2$ by radiorespirometry as described previously [11]. Total isotope release was usually analyzed after one week of incubation at 31°C [9].

Staining of *M.leprae*-infected macrophages: Coverslips of *M.leprae*-infected adherent macrophages were prefixed with absolute methanol and acid-fast stained. The specimens were observed under Nikon Optiphot light microscopy.

Results

Viability of *M.leprae* in mouse macrophages cultured *in vitro*: Mouse peritoneal resident macrophages (1×10^6 cells per well) were incubated with freshly harvested *M.leprae* (multiplicity of infection (MOI), 5:1 or 10:1) for 4 hr to allow phagocytosis. Non-phagocytosed bacilli were washed off and the culture of the macrophages continued for up to 14 days. Viability (metabolic activity) of *M.leprae* in macrophages was assessed by radiorespirometry. As shown in Fig. 1, the viability of the bacilli was gradually decreased in macrophages cultured at 35°C. In contrast, the viability was significantly lost, if the macrophages were cultured at 37°C. Next, the mouse peritoneal

resident macrophages were incubated with 3 doses of *M.leprae* (MOI, 1:1, 4:1 and 10:1) for 4 hr to allow phagocytosis, and the culture continued for longer periods up to 21 days. Viability of *M.leprae* in macrophages was assessed at 7 day intervals. As shown in Fig. 2, in each dose of *M.leprae* infection, decrease in viability was significant after 21 days.

Effects of cytokines on viability of *M.leprae* in mouse macrophages: Supplementation of IL-10 to the infected macrophage culture was

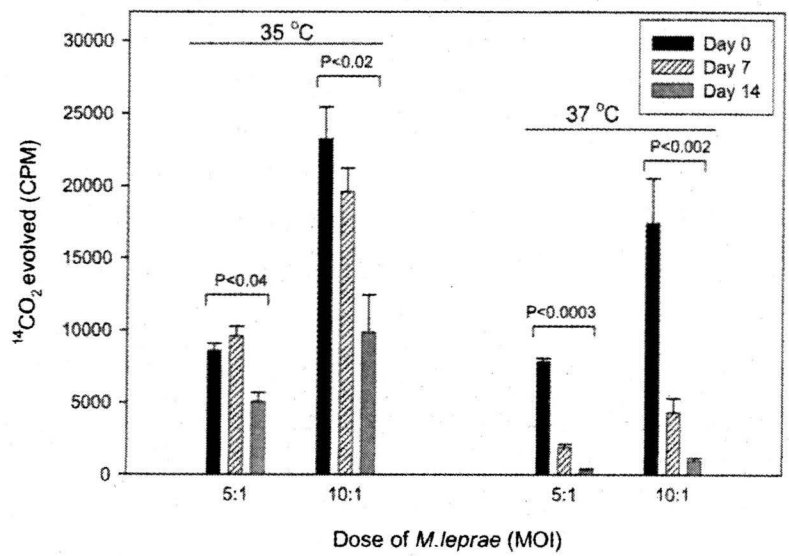

Fig.1. Viability of *M.leprae* in mouse macrophages cultured *in vitro*. Mouse peritoneal resident macrophages were incubated with 5×10^6 or 1×10^7 per well of *M.leprae* (MOI, 5:1 or 10:1), for 4 hr at 37°C to allow phagocytosis. Non-phagocytosed bacilli were washed off and the culture of the macrophages continued up to 14 days at 35°C or 37°C. The cells were lysed to obtain *M.leprae* and metabolism of the bacilli was assessed by radiorespirometry.

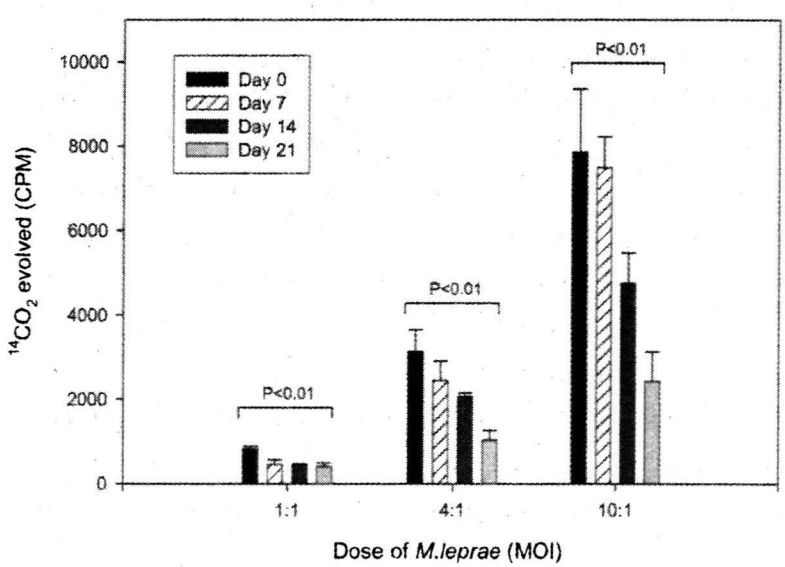

Fig.2. Viability of *M.leprae* in mouse macrophages cultured *in vitro*. Mouse peritoneal resident macrophages were incubated with 3 doses, 1×10^6, 4×10^6 and 1×10^7 per well of *M.leprae* (MOI, 1:1, 4:1 and 10:1) at 35°C for 4 hr to allow phagocytosis, and the culture continued at 35°C for longer periods up to 21 days. The cells were lysed to obtain *M.leprae* and metabolism of the bacilli was assessed by radiorespirometry.

clearly associated with sustained viability of intracellular *M.leprae* cultured at 35°C (Fig.3). In the presence of 3 U/ml of IL-10, *M.leprae* maintained their viability, whereas viability was steadily lost without IL-10. We also examined the effect of TGF-β, another suppressive cytokine for macrophage activation, on the viablility of the bacilli. To the contrary, supplementation of TGF-β

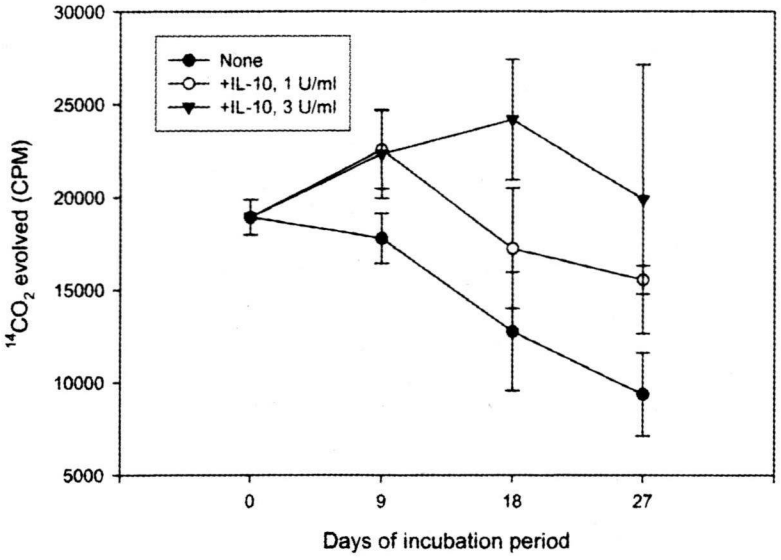

Fig.3. Effect of IL-10 on *M.leprae* survival in mouse macrophages. Mouse peritoneal resident macrophages were incubated with 1×10^7 per well of *M.leprae* (MOI, 10:1) at 35°C for 4 hr to allow phagocytosis, and the culture continued at 35°C for 9, 18 and 27 days. The cells were lysed to obtain *M.leprae* and metabolism of the bacilli was assessed by radiorespirometry.

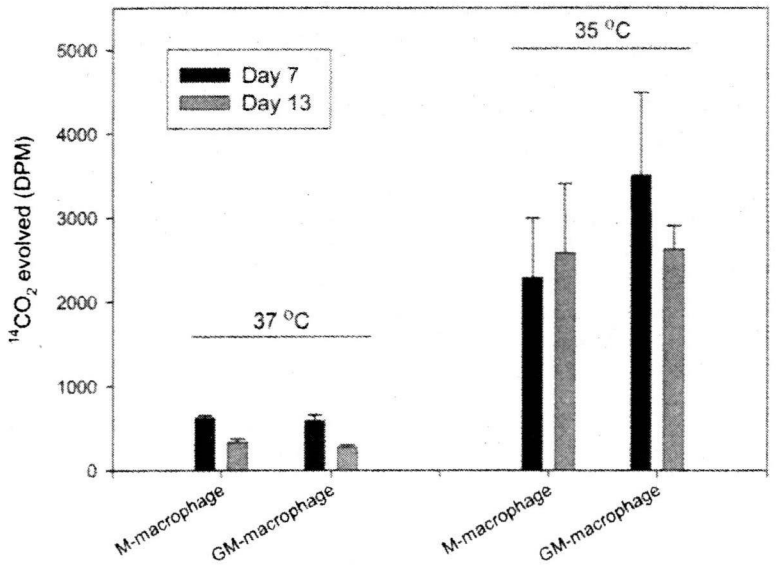

Fig.4. Viability of *M.leprae* in human macrophages cultured *in vitro*. Human M- or GM-macrophages were incubated with *M.leprae* (MOI, 50:1) for 20 hr either at 35°C or 37°C for infection and incubated at the same temperatures for indicated periods. By observation of the acid fast-stained cells under light microscopy, no difference was recognized in the number of *M.leprae* phagocytosed by macrophage cultured between at 35°C and at 37°C. So the viability at day 0 is considered equal. After 7 days and 13 days incubation period, the cells were lysed to obtain *M.leprae* and metabolism of the bacilli was assessed by radiorespirometry (dpm: disintegrations per minute).

significantly decreased the viability of *M.leprae*, when incubated for longer than 28 days post infection (Table 1).

Viability of *M.leprae* in human macrophages cultured *in vitro*: Human macrophages were obtained by culturing monocytes in the presence of either M-CSF or GM-CSF for 7 days. These macrophages (1×10^5 cells per well) were incubated with *M.leprae* (MOI, 50:1) for 20 hr either at 35°C or 37°C for infection and incubated again at the same temperatures. By observation of the acid fast-stained cells under light microscopy,

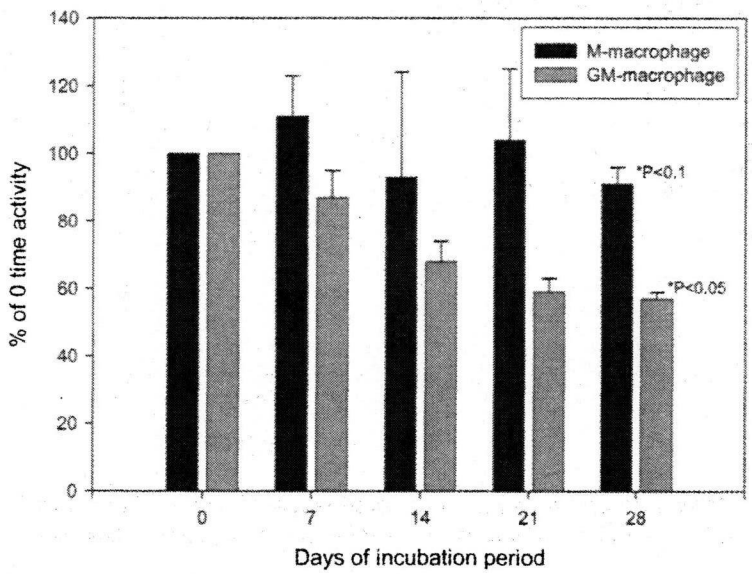

Fig.5. Viability of *M.leprae* in human macrophages cultured *in vitro*. Human M- or GM-macrophages were infected with *M.leprae* (MOI, 50:1) for 20 hr at 35°C and incubated again at 35°C for indicated periods. The cells were lysed to obtain *M.leprae* and metabolism of the bacilli was assessed by radiorespirometry. The results at day 7, 14, 21 and 28 are expressed as percentages of *M.leprae* metabolic activity at time 0. Radiorespirometry data obtained from *M.leprae* in M-macrophages at time 0 was 5,932±399 and those in GM-macrophages was 3,084±78. *P values calculated in comparison to day 0 viability.

Table 1. Effect of TGF-β on survival of *M.leprae* in mouse macrophages cultured at 35°C[a]

Experiment 1				
Days of incubation period	At time 0	7	14	28
Medium only	5,222±936[b]	2,774±295	3,086±425	2,828±1,815
+TGF-β		2,919±535	3,119±1,339	1,973±126

Experiment 2				
Days of incubation period	At time 0	14	28	49
Medium only	26,791±1,428	19,103±621	7,420±2,986	5,713±1,144
+TGF-β		14,306±2,240	3,728±410	1,594±317

[a]Mouse peritoneal resident macrophages were incubated with *M.leprae* (MOI, 1:10) for 4 hr to allow phagocytosis, and the culture continued for indicated periods. The cells were lysed to obtain *M.leprae* and metabolism of the bacilli was assessed by radiorespirometry.
[b]Radiorespirometry data, cpm.
Dose of TGF-β, 500pg/ml.
N.D., not determined.

no difference was recognized in the number of *M.leprae* phagocytosed by macrophage cultured at 35°C and at 37°C (data not shown). Viability of *M.leprae* was assessed after 7 and 13 days. The results clearly showed that the viability of *M.leprae* incubated at 35°C was maintained, whereas the viability was lost if cultured at 37°C (Fig. 4). Next, *M.leprae*-infected human M- and GM-macrophages were cultured for prolonged periods at 35°C. Viability was sustained well for 4 weeks in human macrophages, especially in M-macrophages (Fig. 5).

Discussion

In vivo M.leprae is able to enter and survive in a wide variety of tissues and cell types[12]. The preferred host cell for the leprosy bacillus appears to be the macrophages and a number of unsuccessful attempts have been made to grow *M.leprae* in macrophages *in vitro*. For example, Sharp and Banerjee[13] employed macrophages from conventional mice and rats, *nu/nu* mice or *nu/nu* rats and armadillos. The *M.leprae* inocula were derived from 3 sources (human leproma, *nu/nu* mouse footpad and frozen infected armadillo tissue). Incubation temperature was varied from 31°C to 35°C and *M.leprae*-infected cells were maintained for up to 200 days. Fieldsteel and McIntosh [14] employed a range of rat, mouse and human tissue. The conclusion of these reports is that no significant multiplication of *M.leprae* occurred in any of the cells or tissues.

Previously, we reported that metabolically active *M.leprae* could be maintained in monolayer cultures of mouse peritoneal macrophages and that supplemental IL-10 bolstered *M.leprae* metabolism in the macrophages for as long as 8 weeks. In the cell culture system, temperature is an extremely important factor for growth and 31-33°C incubation temperature is more permissive than 37°C [5]. In the present study, we further observed that incubation of mouse macrophages infected with *M.leprae* at 35°C was also more growth permissive than at 37°C. We chose 35°C as the incubation temperature, and not 31°C, because the maintenance of the integrity of the macrophage monolayer was better at 35°C than at 31-33°C. Moreover, the monolayer of *M.leprae*-infected human macrophages at 31-33°C could not be maintained for longer than one week. We observed that maintenance of the monolayer was good at 35°C, and *M.leprae* at 35°C was also more growth permissive than those at 37°C in human macrophages (Fig. 4 and 5). Our starting inoculum of *M.leprae* was freshly obtained for each experiment from infected *nu/nu* mice. We also were able to rapidly quantify the metabolic activity of *M.leprae* using the radiorespirometry technique adapted by Franzblau [11]. This assay is accurate and highly sensitive with the results available in a short duration of 1 wk (compared to 6-12 months when titrated in mouse footpads). Radiorespirometry data correlates well with other *in vitro* systems [11] but, more importantly, the data correlated well with "viability" as observed in the mouse footpad system [12].

Various clinical evidence suggests that *M.leprae* prefer a growth temperature of less than 37°C [1]. In animal models, *M.leprae* multiplies in the mouse foot pad where the temperature is lower than the body temperature [2]. In addition, *Dasypus novemcinctus*, the nine-banded armadillo has a core temperature of ~33°C, which renders it permissive as a host for the leprosy bacillus [13]. Mononuclear phagocytes in virtually every organ of the natural or experimentally infected armadillo become heavily parasitized with propagating *M. leprae* [14]. Whether intracellular or extracellular, *M.leprae* clearly prefers temperatures cooler than

normal human body temperature [12], and 37°C appeared to be highly detrimental to *M.leprae* viability. The *in vitro* results obtained in the present study confirmed the preference of lower temperature (35°C) by *M.leprae* residing in human macrophages.

In this study, supplemental IL-10, but not TGF-β supported the metabolic activity of *M.leprae* in mouse macrophages for several weeks, similar to the results obtained previously [5]. In choosing TGF-β and IL-10 as the cytokines that might bolster the intracellular survival of *M.leprae,* we were attempting to down-regulate any innate ability of the normal macrophages to cope with the organism. TGF-β is produced by activated macrophages and other inflammatory cells and has a broad array of modulatory functions on the immune response. TGF-β has been shown to interfere with macrophage antimicrobial mechanisms including the generation of reactive oxygen intermediates [15] and reactive nitrogen intermediates [16], and has been shown to enhance the intracellular growth of *M.tuberculosis* in human monocytes [17]. However, in the present studies with mouse macrophages, exogenous TGF-β had no detectable effect on sustaining intracellular *M.leprae* viability, and in fact decreased the viability (Table 1). In contrast, supplementing media with IL-10 clearly affected the long term viability of *M.leprae* in mouse macrophages (Fig. 3). IL-10 is produced by T cells, B cells and macrophages [18, 19]. IL-10 has been shown to be a potent down-regulator of cell-mediated immunity to intracellular pathogens [20]. *In vivo*, endogenous IL-10 dampened the cell-mediated immune response to avirulent mycobacterial infection [4] and appeared to lead to loss of control of *M.tuberculosis* infection with widespread dissemination [21]. IL-10 functions in part at the level of the macrophage by attenuating iNOS mRNA expression, iNOS activity and, by inference, NO production [22]. In human macrophages, however, the viability of *M.leprae* was maintained for 4 weeks in the absence of IL-10 (Fig. 5), suggesting that human cells seem to be better hosts than mouse cells for *M.leprae* survival. Viability of *M.leprae* in M-macrophages seems to be maintained for a longer period (up to one month) than that in GM-macrophages (Fig. 5). One of the reasons for this may be due to the production of IL-10 by M-macrophages [23], although the mechanism by which IL-10 contributes to the maintenance and growth of *M.leprae* is unclear.

In conclusion, the present study showed that the metabolism, and presumably the viability, of *M.leprae* could be sustained under culture conditions at 35°C, which is also a moderate temperature necessary to maintain the integrity of macrophages.

Acknowledgments

The study was supported partly by a Health Science Research Grant of Emerging and Re-emerging Infectious Diseases, from the Ministry of Health, Labour and Welfare of Japan. We are also grateful to the Japanese Red Cross Society for kindly providing PBMCs from healthy donors.

References

1) Brand PW: Temperature variation and leprosy deformity. Int J Lepr 27:1-7, 1959.
2) Shepard CC: Temperature Optimum of *Mycobacterium leprae* in Mice. J Bacteriol 90:1271-1275, 1965.
3) Yamamura M, Uyemura KD, Aeans RJ, Weinberg K, Rea TH, Bloom.BR, Modlin RL: Defining protective response to pathgens: cytokine profiles in leprosy lesions. Science 254:277-282, 1991.

4) Sharma S, Bose M: Role of cytokines in immune response to pulmonary tuberculosis. Asian Pac J Allergy Immunol 19: 213-219, 2001.

5) Fukutomi Y, Matsuoka M, Minagawa F, Toratani S, McCormick G, Krahenbuhl J: Subversion of macrophage anti-microbial function bolsters intracellular survival of *M.leprae*. Int J Lepr 72:16-26, 2004.

6) Kohsaka K, Mori T, Ito T: Lepromatoid lesion developed in nude mouse inoculated with *Mycobacterium leprae*. Lepro 45:177-187, 1976.

7) Nakamura M: Elimination of contaminants in a homogenate of nude-mouse footpad experimentally infected with *Mycobacterium leprae*. Jpn J Lepr 64:47-50, 1994.

8) Shepard CC, McRae DH: A method for counting acid-fast bacteria. Int J Lepr 36:78-82, 1968.

9) Adams LB, Franzblau S, Taintor R, Hibbs J Jr, Krahenbuhl JL: L- arginine-dependent macrophage effector functions inhibit metabolic activity of *Mycobacterium leprae*. J Immunol 147: 1642- 1646, 1991.

10) Maeda Y, Mukai T, Spencer J, Makino M: Identification of an immunomodulating agent from *Mycobacterium leprae*. Infect Immun 73:2744-2750, 2005.

11) Franzblau SG: Oxidation of palmitic acid by *Mycobacterium leprae* in an axenic medium. J Clin Microbiol 2618-2624, 1988.

12) Truman RW, Krahenbuhl JL: Viable *Mycobacterium leprae* as a research reagent. Int J Lepr 69: 1-12, 2001.

13) Kirchheimer W F, Storrs EH: Attempts to establish the armadillo (*Dasypus novemcinctus*) as a model for the study of leprosy. Int J Lepr 39:693-702, 1971.

14) Fieldsteel AH, McIntosh AH: Attempts to cultivate and determine the maximum period of viability of *M.leprae* in tissue culture. Int J Lepr 40: 271-277, 1972.

15) Tsunawaki S, Sporn M, Ding A, Nathan C: Deactivation of macrophage by transforming growth factor-beta. Nature 334:260-262, 1988.

16) Ding A, Nathan CF, Graycar J, Derynck R, Stuehr DJ, Srimal S: Macrophage deactivating factor and transforming growth factors-beta 1, - beta 2 and -beta 3 inhibit induction of macrophage nitrogen oxide synthesis by IFN-gamma. J Immunol 145:940-944, 1990.

17) Hirsch CS, Yoneda T, Averill L, Ellner JJ, Toosi Z: Enhancement of tintracellular growth of *Mycobacterium tuberculosis* in human monocytes by transforming growth factor-1. J Inf Dis 170:1229-1237, 1994.

18) Fiorentino DF, Zlotnik A, Viera P, Mosmann TR, Howard M, Moore KW, O'Garra A: IL-10 acts on the antigen presenting cell to inhibit cytokine production by Th1 cells. J Immunol 146:3444-3451, 1991.

19) O'Garra A, Chang R, Go N, Hastings R, Haughton G, Howard M: Ly-1 B (B-1) cells are the main source of B cell - derived IL-10. Eur J Immunol 22:711-717, 1992.

20) Redpath S, Ghazal P, Gascoigne NR: Hijacking and exploitation of IL-10 by intracellular pathogens. Trends Microbiol 9:86-92, 2001.

21) Dugas N, Palacios-Calender M, Dugas B, Riveros-Moreno V, Delfraissy J, Kolb J, Moncada S: Regulation by endogenous IL-10 of the expression of nitric oxide synthase induced by ligation of CD23 in human macrophage. Cytokine 10:680-689, 1998.

22) Huang C, Stevens B, Nielsen E, Slovin P, Fang X, Nelson D, Skimming J: Interleukin-10 inhibition of nitric oxide biosynthesis involves suppression of CAT-2 transcription. Nitric Oxide 6:79-84, 2002.

23) Makino M, Maeda Y, Fukutomi Y, Mukai T: Contribution of GM-CSF on the enhancement of the T cell-stimulating activity of macrophages. Microbes Infect 91:70-77, 2007.

Vaccine 27 (2009) 3267–3270

Contents lists available at ScienceDirect

Vaccine

journal homepage: www.elsevier.com/locate/vaccine

Novel prophylactic and therapeutic vaccine against tuberculosis

Masaji Okada[a,*], Yoko Kita[a], Toshihiro Nakajima[b], Noriko Kanamaru[a], Satomi Hashimoto[a], Tetsuji Nagasawa[b], Yasufumi Kaneda[c], Shigeto Yoshida[d], Yasuko Nishida[a], Hitoshi Nakatani[a], Kyoko Takao[a], Chie Kishigami[a], Yoshikazu Inoue[a], Makoto Matsumoto[e], David N. McMurray[f], E.C. dela Cruz[g], E.V. Tan[g], R.M. Abalos[g], J.A. Burgos[g], Paul Saunderson[g], Mitsunori Sakatani[a]

[a] Clinical Research Center, National Hospital Organization Kinki-chuo Chest Medical Center, 1180 Nagasone, Kitaku, Sakai, Osaka 591-8555, Japan
[b] Ikeda Laboratory, GenomIdea Inc.,1-8-31 Midorigaoka, Ikeda, Osaka 530-0043, Japan
[c] Division of Gene Therapy Science, Graduate School of Medicine, Osaka University, 2-2 Yamadaoka, Suita, Osaka 565-0871, Japan
[d] Department of Medical Zoology, Jichi-Med. Sch., 3311-1 Yakushiji, Minamikawachi-machi, Tochigi 329-0498, Japan
[e] Otsuka Pharmaceutical Co. Ltd., 463-10 Kagasuno, Kawauchi-cho, Tokushima 771-0192, Japan
[f] Texas A & M University, System Health Science Center, College of Medicine, College Station, TX 77843-1114, USA
[g] Leonard Wood Memorial, Jagobiao, Mandaue City, Cebu 6000, Philippines

ARTICLE INFO

Article history:
Available online 5 February 2009

Keywords:
HSP65 + IL-12 DNA vaccine
Tuberculosis
Therapeutic effect

ABSTRACT

We have developed a novel tuberculosis (TB) vaccine; a combination of the DNA vaccines expressing mycobacterial heat shock protein 65 (HSP65) and interleukin 12 (IL-12) delivered by the hemagglutinating virus of Japan (HVJ)-envelope and -liposome (HSP65 + IL-12/HVJ). This vaccine provided therapeutic efficacy as well as remarkable protective efficacy via $CD8^+$ T and $CD4^+$ T cells in murine models compared with the saline controls, on the basis of CFU of number of multi-drug resistant TB (MDR-TB), and survival of extremely drug resistant TB (XDR-TB) challenged mice. Furthermore, we extended our studies to a cynomolgus monkey model, which is currently the best animal model of human tuberculosis. This vaccine exerted therapeutic efficacy (survival and immune responses) in the TB-infected monkeys. These data indicate that our novel DNA vaccine might be useful against *Mycobacterium tuberculosis* including XDR-TB and MDR-TB for human therapeutic clinical trials.

1. Introduction

Tuberculosis is a major global threat to human health, with about 2 million people dying every year from *Mycobacterium tuberculosis* (TB) infection. The only tuberculosis vaccine currently available is an attenuated strain of *Mycobacterium bovis* BCG (BCG), although its efficacy against adult TB disease remains controversial. Furthermore, multi-drug resistant tuberculosis (MDR-TB) and extremely drug resistant TB (XDR-TB) are becoming big problems in the world. In such circumstances, the development of therapeutic vaccine against TB as well as prophylactic vaccine against TB is required. Therefore, we have recently developed a novel TB vaccine, a DNA vaccine expressing mycobacterial heat shock protein 65 (HSP65) and interleukin-12 (IL-12) delivered by the hemagglutinating virus of Japan (HVJ)-liposome (HSP65 + IL-12/HVJ). This vaccine was 100-fold more efficient than BCG in the murine model on the basis of the elimination of *M. tuberculosis* mediated by the induction of CTL [1,2]. A nonhuman primate model of TB will provide information for vaccine development. In fact, in the previous study we evaluated the protective efficacy of HSP65 + IL-12/HVJ in the cynomolgus monkey model, which is an excellent model of human tuberculosis [1,3]. Furthermore, we observed the synergistic effect of the HSP65 + IL-12/HVJ and BCG using a priming-booster method in the TB-infected cynomolgus monkeys. The combination of the two vaccines showed a very strong prophylactic efficacy against *M. tuberculosis* (100% survival) as we have seen previously in the murine model of TB [4]. In the present study, we evaluated therapeutic effect and prophylactic effect of this vaccine on the MDR-TB infection and XDR-TB infection in murine and monkey models.

2. Materials and methods

DNA vaccines encoding *M. tuberculosis* HSP65 and human IL-12 were encapsulated into HVJ-envelope or HVJ-liposomes [5]. CTL activity was assessed by ^{51}Cr-release [1,6].

At 5 and 10 weeks after intravenous challenge of *M. tuberculosis* H37RV, the number of CFU in the lungs, spleen, and liver were counted and therapeutic efficacy of HVJ-envelope DNA vaccines was evaluated [1]. Therapeutic efficacy was also evaluated by chronic TB infection model of mice using aerosol challenge of TB

* Corresponding author. Tel.: +81 72 252 3021; fax: +81 72 251 2153.
E-mail address: okm@kch.hosp.go.jp (M. Okada).

0264-410X/$ – see front matter © 2009 Elsevier Ltd. All rights reserved.
doi:10.1016/j.vaccine.2009.01.064

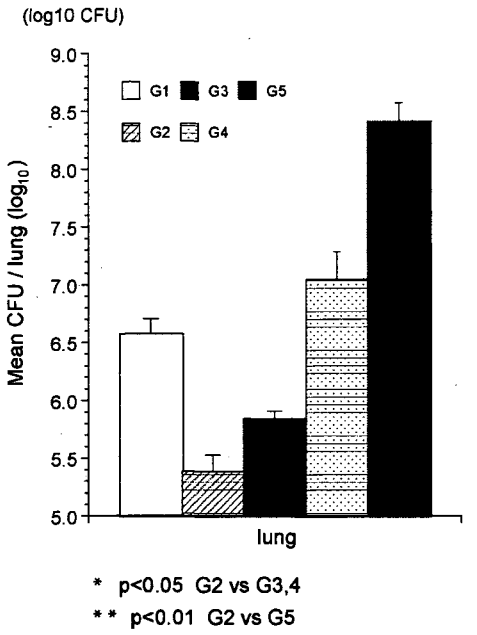

Fig. 1. The *in vivo* necessity of CD8 positive T cells and CD4 positive T cells for prophylactic efficacy of the HVJ-envelope/HSP65 DNA + IL-12 DNA vaccine. Anti-CD8 antibody and/or anti-CD4 antibody were injected i.p. every 5 days after the challenge of TB. BCG was used as a priming vaccine and this DNA vaccine was immunized 2 times (HVJ-envelope/HSP65 DNA 50 μg + IL-12 DNA 50 μg) as booster vaccine. 4 weeks after last immunization, 5×10^5 H37RV were challenged i.v. into mice. G1: without vaccine (□). G2: vaccine (▨). G3: vaccine + anti-CD8 antibody (■). G4: vaccine + anti-CD4 antibody (⊠). G5: vaccine + anti-CD8 antibody + anti-CD4 antibody (■) (G2–G3: $P<0.05$) (G2–G4: $P<0.05$) (G2–G5: $P<0.01$).

(15 CFU/mouse: Madison aerosol exposure chamber, University of Wisconsin). 5 weeks after aerosol infection of TB, the vaccine was administered to mice 6 times in 3 weeks.

Cynomolgus monkeys were housed in a BL 3 animal facility of the Leonard Wood Memorial Research Center. The animals were vaccinated 9 times with the HVJ-envelope with expression plasmid of both HSP65 and human IL-12 (HSP65 + hIL-12/HVJ: 400 μg i.m.), 1 week after the challenge with the *M. tuberculosis* Erdman

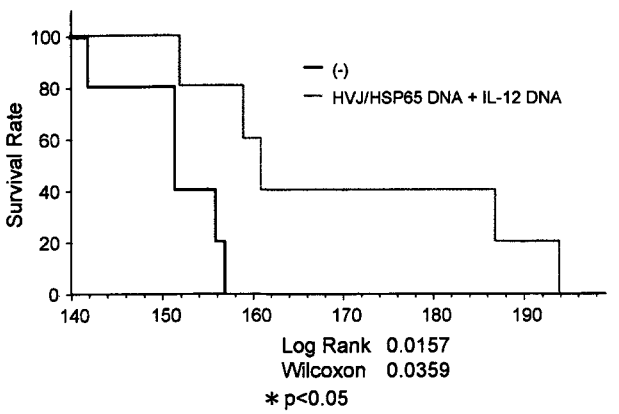

Fig. 2. Therapeutic efficacy of HVJ-envelope/HSP65 DNA + IL-12 DNA vaccine on the extremely drug resistant *Mycobacterium tuberculosis* (XDR-TB). The survival of DBA/1 mice treated with HVJ-envelope/HSP65 DNA (50 μg) + IL-12 DNA vaccine (50 μg) 3 times after 5×10^5 XDR-TB, injection i.v. XDR-TB is resistant to RFP, INH, SM, EB, KM, EVM, TH, PAS, LEFX and PZA. XDR-TB is only sensitive to CS. Survival rate of mice treated with HVJ-envelope/HSP65 DNA + IL-12 DNA (■). Survival rate of control mice without treatment (■). Kaplan–Meier's method (log rank test and Wilcoxon) was used to compare the survival of each group (G1–G2: log rank 0.0157 Wilcoxon 0.0359).

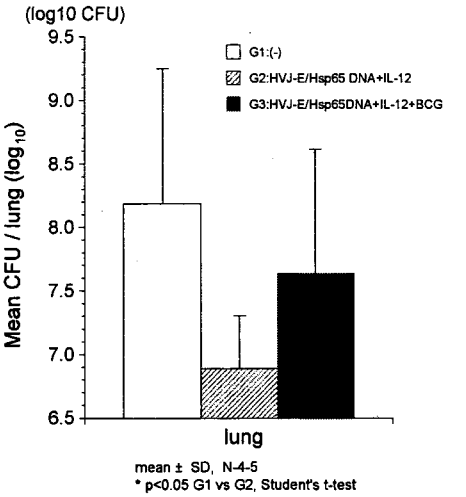

Fig. 3. Therapeutic efficacy of HVJ-envelope/HSP65 DNA + IL-12 DNA vaccine on MDR-TB TNF R gene disrupted DBA/1 mice were treated with HVJ-envelope/HSP65 DNA + IL-12 DNA vaccine 3 times after 5×10^5 MDR-TB injection i.v. CFU of MDR-TB in the lungs of mice, 4 weeks after MDR-TB injection, were assessed as described in Section 2. G1: (−) (□). G2: treated with HVJ-envelope/HSP65 DNA + IL-12 DNA (▨). G3: treated with HVJ-envelope/HSP65 DNA + IL-12 DNA and BCG (■). Student's *t*-test was used to compare the CFU of TB of each group (G1–G2: $P<0.05$).

strain (5×10^2) by intratracheal instillation. Immune responses and survival were examined as described in our previous studies [2,4].

3. Results

The purpose of this study was to elucidate the therapeutic efficacy of a TB vaccine we have developed in a murine and nonhuman primate TB model [1,3].

The *in vivo* necessity of CD8 positive T cells as well as CD4 positive T cells to exert the prophylactic efficacy of the HVJ-

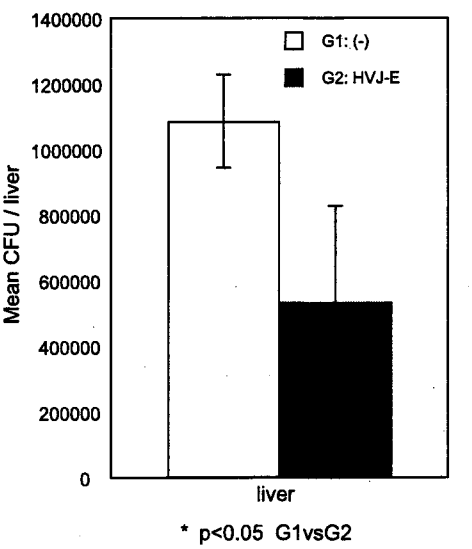

Fig. 4. Therapeutic efficacy of HVJ-envelope/HSP65 DNA + IL-12 DNA, using *in vivo* humanized immune models of IL-2 receptor γ-chain disrupted NOD-SCID mice (SCID-PBL/hu). Groups of animals were treated with 3 times with HVJ-envelope/HSP65 DNA + IL-12 DNA (50 μg i.m.) 10 days after the third vaccination, mice were sacrificed and CFU of TB in the liver of mice were accessed as described in Section 2 (1, 2). 1×10^7 PBL from a healthy human volunteer were injected i.p. into IL-2 receptor γ-chain disrupted NOD-SCID mice. 21 days after injection of PBL, mice were challenges with 5×10^5 H37RV i.v. and then treated with the vaccine. G1: (−) control (□). G2: treated with HVJ-envelope/HSP65 DNA + IL-12 DNA (■). Student's *t*-test was used to compare the CFU of TB of each group (G1–G2: $P<0.05$).

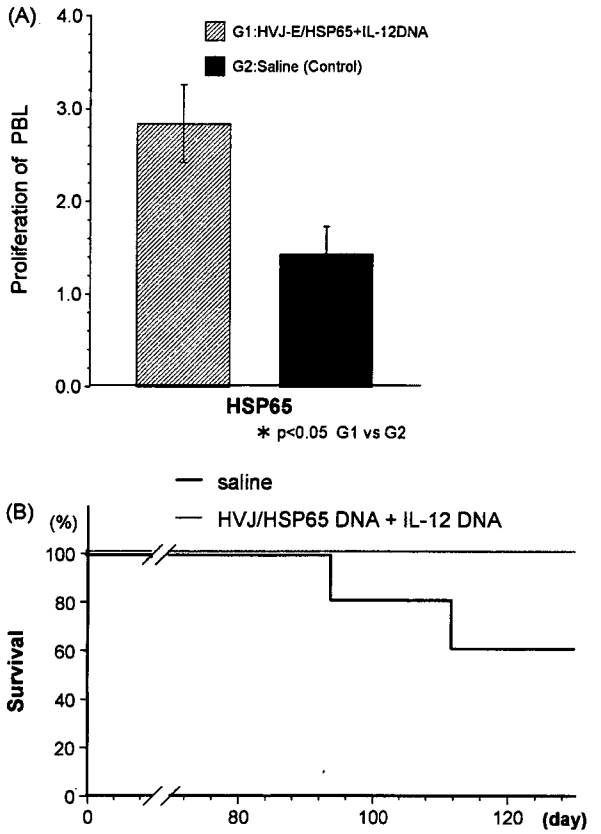

Fig. 5. (A) Therapeutic efficacy of HVJ-envelope/HSP65 DNA + IL-12 DNA vaccine using cynomolgus monkey. Five cynomolgus monkeys were treated with HVJ-envelope/HSP65 DNA + IL-12 DNA vaccine 9 times after 5×10^2 MTB intratracheal instillation. Stimulation index of the proliferation of PBL from these monkeys and that from five control monkeys (saline injected) were assessed by the stimulation with HSP65 antigen. G1: HVJ-envelope/HSP65 DNA + IL-12 DNA treatment (▨). G2: saline (control) (■). Tukey–Kramer's HSD tests were used to compare proliferative responses of PBL between groups (G1–G2: $P < 0.05$). (B) Survival periods of 5 monkeys treated with HVJ-envelope/HSP65 DNA + IL-12 DNA vaccine 9 times after TB challenge were shown (■). Survival periods of 5 monkeys treated with saline (control) were shown (■).

envelope/HSP65 DNA + IL-12 DNA vaccine was demonstrated in mice. Anti-CD8 antibody alone or anti-CD4 antibody alone treatment during the whole immunization period induced the increase in the number of TB in the mice immunized with the vaccine (Fig. 1). Both anti-CD8 antibody and anti-CD4 antibody treatment increased in the number of TB synergistically.

Fig. 2 shows the survival of vaccinated mice after XDR-TB (extremely drug resistant TB). All mice in the control group died of TB within 160 days after XDR-TB infection. In contrast, mice treated with HVJ-envelope/HSP65 DNA + IL-12 DNA prolonged the survival periods significantly by statistical analysis ($P < 0.05$). It was demonstrated that this vaccine had a therapeutic activity against XDR-TB.

At 5 and 10 weeks after intravenous challenge of MDR-TB, the CFU in the lungs, spleen, and liver were counted and therapeutic efficacy of HVJ-envelope DNA vaccine was evaluated.

As shown in Fig. 3, HVJ-Env/HSP65 DNA + IL-12 DNA vaccine treatment significantly reduced the bacterial loads as compared to saline control group ($P < 0.05$).

Therapeutic efficacy of HVJ-envelope/HSP65 DNA + IL-12 DNA was also observed, using in vivo humanized immune models of IL-2 receptor γ-chain disrupted NOD-SCID mice constructed with human PBL (SCID-PBL/hu) [7,8].

Fig. 4 shows the results of bacterial loads 5 weeks after TB infection. Therapeutic vaccination with HVJ-Env/HSP65 DNA + IL-12 DNA group resulted in significantly therapeutic activity even in SCID-PBL/hu mice which exerted human T cell immune responses.

Furthermore, the therapeutic activity of this vaccine was evaluated in a nonhuman primate model infected with *M. tuberculosis*.

Fig. 5A shows the results of immune responses of cynomolgus monkey at 11 weeks after challenge of *M. tuberculosis* Erdman strain (5×10^2) by intratracheal instillation. The proliferation of PBL in therapeutic vaccination of monkeys in the group with HVJ-Env/HSP65 DNA + IL-12 DNA was augmented. This vaccine also improved the survival of monkeys, compared to the saline (control) group, during the period between 0 weeks and 19 weeks after TB challenge (Fig. 5B).

4. Discussion

The HSP65 + hIL-12/HVJ vaccine exerted a significant therapeutic effect against TB, as indicated by: (1) extension of survival of mice infected with XDR-TB, (2) decrease in the CFU of TB in lungs, liver and spleen of mice infected with MDR-TB as well as drug-sensitive TB (H37RV), (3) decrease in the CFU of TB in these organs of mice challenged with TB in the *in vivo* humanized immune model of SCID-PBL/hu and (4) augmentation of immune responses, in a cynomologus monkey model which closely mimics human TB disease. It is important to evaluate the survival of monkey [6,7]. During the period between 0 weeks and 19 weeks after TB challenge, increase in the survival rate of the monkeys treated with this vaccine were observed, compared to the control monkeys treated with saline.

MDR-TB and XDR-TB are becoming big problems in the world. About 500,000 new patients with MDR-TB are shown every year. However, the effective drugs against MDR-TB are few.

The HVJ-envelope/HSP65 DNA + IL-12 DNA vaccine exerted the therapeutic activity even against XDR-TB, which is resistant to RFP, INH, SM, EB, KM, EVM, TH, PAS, LEFX and PZA and only sensitive to CS. Thus, our results with the HVJ-envelope/HSP65 DNA + IL-12 DNA vaccine in the murine therapeutic model and cynomologus monkey therapeutic model should provide a significant rationale for moving this vaccine into clinical trial. Furthermore, we have established chronic TB disease model using mouse infected with TB in the aerosol chamber (data not shown) [9]. By using this model, therapeutic efficacy of this vaccine was also observed.

Thus, we are taking advantage of the availability of multiple animal models to accumulate essential data on the HVJ-envelope DNA vaccine in anticipation of a phase I clinical trial.

Acknowledgements

This study was supported by a Health and Labour Science Research Grant from MHLW (H11-shinko-2, H14-shinko-1, H17-shinko-5, H20-shinko-14), international collaborative study grants from Human Science foundation and Grant-in-Aid for Scientific Research(B) from the Ministry of Education, Culture, Sports, Science and Technology Japan, and Grant of Osaka Tuberculosis Foundation.

References

[1] Yoshida S, Tanaka T, Kita Y, Kuwayama S, Kanamaru N, Muraki Y, et al. DNA vaccine using hemagglutinating virus of Japan-liposome encapsulating combination encoding mycobacterial heat shock protein 65 and interleukin-12 confers protection against *Mycobacterium tuberculosis* by T cell activation. Vaccine 2006;24:1191–204.

[2] Okada M, Kita Y, Nakajima T, Kanamaru N, Hashimoto S, Nagasawa T, et al. Evaluation of a novel vaccine (HVJ-liposome/HSP65 DNA+IL-12 DNA) against tuberculosis using the cynomologus monkey model of TB. Vaccine 2007;25(16):2990–3.

[3] Walsh GP, Tan EV, dela Cruz EC, Abalos RM, Villahermosa LG, Young LJ, et al. The Philippine cynomolgus monkey provides a new nonhuman primate model of tuberculosis that resembles human disease. Nat Med 1996;2(4):430–6.

[4] Kita Y, Tanaka T, Yoshida S, Ohara N, Kaneda Y, Kuwayama S, et al. Novel recombinant BCG and DNA-vaccination against tuberculosis in a cynomolgus monkey model. Vaccine 2005;23:2132–5.
[5] Saeki Y, Matsumoto N, Nakano Y, Mori M, Awai K, Kaneda Y. Development and characterization of cationic liposomes conjugated with HVJ (Sendai virus). Hum Gene Ther 1997;8(17):2133–41.
[6] Okada M, Yoshimura N, Kaieda T, Yamamura Y, Kishimoto T. Establishment and characterization of human T hybrid cells secreting immunoregulatory molecules. Proc Natl Acad Sci USA 1981;78(12):7717–21.
[7] Okada M, Okuno Y, Hashimoto S, Kita Y, Kanamaru N, Nishida Y, et al. Development of vaccines and passive immunotherapy against SARS corona virus using SCID-PBL/hu mouse models. Vaccine 2007;25:3038–40.
[8] Tanaka F, Abe M, Akiyoshi T, Nomura T, Sugimachi K, Kishimoto T, et al. The anti-human tumor effect and generation of human cytotoxic T cells in SCID mice given human peripheral blood lymphocytes by the *in vivo* transfer of the interleukin-6 gene using adenovirus vector. Cancer Res 1997;57(7):1335–43.
[9] Flynn JL, Chan J. Immunology of tuberculosis. Annu Rev Immunol 2001;19:93–129.

Biochemical and Biophysical Research Communications 387 (2009) 272–277

Contents lists available at ScienceDirect

Biochemical and Biophysical Research Communications

journal homepage: www.elsevier.com/locate/ybbrc

Dissection of Rab7 localization on *Mycobacterium tuberculosis* phagosome

Shintaro Seto [a], Sohkichi Matsumoto [b], Isamu Ohta [c], Kunio Tsujimura [a], Yukio Koide [a,*,1]

[a] Department of Infectious Diseases, Hamamatsu University School of Medicine, 1-20-1 Handa-yama, Higashi-ku, Hamamatsu 431-3192, Japan
[b] Department of Bacteriology, Osaka City University Graduate School of Medicine, 1-4-3 Asahi-machi, Abeno-ku, Osaka 545-8585, Japan
[c] Research Equipment Center, Hamamatsu University School of Medicine, 1-20-1 Handa-yama, Higashi-ku, Hamamatsu 431-3192, Japan

ARTICLE INFO

Article history:
Received 16 June 2009
Available online 4 July 2009

Keywords:
Macrophage
Mycobacterium tuberculosis
Rab7
Phagosome maturation
Phagolysosome biogenesis

ABSTRACT

The late endosomal marker Rab7 has been long believed to be absent from the phagosome containing *Mycobacterium tuberculosis* (*M.tb*) in macrophage, but the detail kinetics remains elusive. Here, we found that Rab7 is transiently recruited to and subsequently released from *M.tb* phagosomes. For further understanding of the effect of Rab7 dissociation from the phagosome, we examined the localization of lysosomal markers on the phagosome in the macrophage expressing a dominant-negative Rab7. The localization of lysosomal associated membrane protein-2 (LAMP-2) on the phagosome was Rab7-independent, while that of cathepsin D was Rab7-dependent. These results agree with the localization of each lysosomal marker on *M.tb* phagosome at 6 h postinfection-*i.e.*, LAMP-2, but not cathepsin D localized on the majority of *M.tb* phagosomes. These results suggest that the dissociation of Rab7 from *M.tb* phagosome is the important process in inhibition of phagolysosome biogenesis.

Introduction

Engulfment of pathogens by macrophages is an important initial step in the innate immune response. Pathogens phagocytosed by macrophages are enclosed into phagocytic vacuoles and processed by a series of interactions with endosome vesicles. This well-known process is called phagosome maturation. During the maturation process, phagosomes acquire degradative and microbicidal properties and undergo phagolysosome biogenesis by fusing with lysosomes. Several proteins, including Rab GTPase proteins, play pivotal roles in phagosome maturation and phagolysosome biogenesis [1]. Rab5 is associated with early phagosomes followed by recruitment of its effector proteins EEA1 and Class III phosphatidylinositol 3-kinase [2]. Rab7 appears on the phagosome membrane after Rab5 dissociation and resides there during the subsequent phagosome maturation [3]. Rab7 regulates the transportation and fusion of late endosomes and lysosomes [1] and has been implicated in the interaction between phagosomes and late endosomal compartments [4].

Mycobacterium tuberculosis (*M.tb*) is a causative pathogen of tuberculosis and has the ability to survive and proliferate in macrophages by blocking phagolysosome biogenesis [5,6]. In the current model of *M.tb*-induced inhibition of phagolysosome biogenesis, phagosome maturation is arrested at the stage of Rab5-Rab7 conversion [7] on *M.tb* phagosomes, leading to the inhibition of phagolysosome biogenesis [8]. This hypothesis is supported by observations that Rab7 is absent from mycobacterial phagosomes in macrophages [9,10]. However, the model was challenged by an observation that *M.tb* phagosomes are associated with lysosomal markers in the early stage of infection, suggesting that *M.tb* phagosomes fuse with lysosomes [11]. These conflicting observations indicate that more precise studies are necessary, particularly studies focusing on the kinetics of Rab7 localization during *M.tb*-induced inhibition of phagolysosome biogenesis. We therefore investigated the temporal and spatial localization of Rab7 in *M.tb*-infected macrophages, together with that of lysosomal markers, lysosomal associated membrane protein-2 (LAMP-2) and cathepsin D. In this study, we demonstrated that Rab7 is transiently recruited to *M.tb* phagosome, after which *M.tb* promotes the dissociation of Rab7 from the phagosome, suggesting that the dissociation of Rab7 limits the subsequent recruitment of cathepsin D and results in the blocking of phagolysosome biogenesis.

Materials and methods

Cell and bacterial cultures. Raw264.7 macrophage was obtained from the American Type Culture Collection and maintained in Dulbecco's modified Eagle's medium (DMEM; Sigma–Aldrich) supplemented with 10% fetal bovine serum (FBS; Thermo Trace), 25 μg/ml penicillin G, and 25 μg/ml streptomycin at 37 °C under 5% CO_2. *M. tuberculosis* H37Rv was grown to mid-logarithmic phase in 7H9 medium supplemented with 10% Middlebrook ADC (BD Bio-

* Corresponding author. Fax: +81 53 435 2101.
E-mail address: koidelb@hama-med.ac.jp (Y. Koide).
[1] Address: Executive director, Hamamatsu University School of Medicine, 1-20-1 Handa-Yama, Higashi-ku, Hamamatsu 431-3192, Japan

0006-291X/$ - see front matter © 2009 Elsevier Inc. All rights reserved.
doi:10.1016/j.bbrc.2009.06.152

sciences), 0.5% glycerol and 0.05% Tween 80 (*Mycobacterium* complete medium) at 37 °C. *M.tb* transformed with a plasmid encoding DsRed [12] was grown in *Mycobacterium* complete medium containing 25 μg/ml kanamycin. *Staphylococcus aureus* was grown in brain heart infusion broth (BD Biosciences) at 37 °C.

Antibodies. Rabbit anti-Rab7 polyclonal antibody (Sigma–Aldrich), rat anti-mouse LAMP-2 monoclonal antibody (SouthernBiotech), goat anti-mouse cathepsin D polyclonal antibody (R&D systems), rabbit anti-cytochrome C polyclonal antibody (Cell Signaling), mouse anti-GFP monoclonal antibody (TaKaRa Bio) were all purchased. Alexa488- and Alexa546-conjugated anti-IgG antibodies (Invitrogen) and 10-nm gold particle-conjugated anti-mouse IgG antibody (EY Laboratories) were purchased.

Plasmid constructs and transfection. Human Rab7 was amplified by PCR using cDNA derived from HeLa cells as a template and primers CAGATCTATGACCTCTAGGAAGAAAGTGTTGCTG and CGAATTCAGCAACTGCAGCTTTCTGCCG. PCR product of Rab7 was inserted into the pEGFP-C1 (Invitrogen). A constitutive-active and a dominant-negative Rab7 mutant were made by site-directed mutagenesis using the Quick-Change site-directed mutagenesis kit (Stratagene), as previously reported [13]. Three million Raw264.7 cells were transfected with 15 μg of plasmid DNA using an MP-100 electroporator (Digital Bio Technology) according to the manufacturer's instructions. Transfected cells were incubated in DMEM with 10% FBS for 24 h before the start of experiments.

Infection of bacteria. Transfected cells grown on round coverslips in 12-well plates were infected with bacteria. Bacterial cells were washed with PBS containing 0.05% Tween 80 three times and suspended in DMEM with 10% FBS at a multiplicity of infection (MOI) of 10–30. Aliquots of 1 ml of bacterial suspension were added to transfected Raw264.7 cells on coverslips in 12-well plates, followed by centrifugation at 150g for 5 min and incubation for 10 min at 37 °C. Infected cells on coverslips were washed with DMEM three times to remove non-infected bacteria, and then incubated with DMEM containing 10% FBS. At the indicated time points, infected cells were fixed with 1% or 3% paraformaldehyde in PBS.

Confocal microscopy. Imaging of cells was performed with a CSU LiveStage LS-1 confocal microscope system (Yokogawa). Four-dimensional (4D) live microscopy was performed with a CSU LiveStage LS-1 confocal microscope system as described previously [14] with modifications. Transfected Raw264.7 cells grown on a 35-mm glass base dish were infected with *M.tb* expressing DsRed. Synchronous infection was performed with centrifugation, washing with DMEM, and incubation with DMEM containing 10% FBS and 20 mM HEPES (pH7.3) without phenol red. Temperature control of the infected cells was carried out by an Onpu-4 incubation system (Taiei-denki). Serial confocal sections (1.5 μm) within a z-stack spanning a total thickness of 20 μm were taken every 5 min from 30 to 155 min after infection. Images with infected bacteria in transfected macrophage cells were chosen from the z-stacks at each time point to make a time-lapse sequence.

Immunoelectron microscopy. *M.tb*-infected macrophages were fixed with 3% paraformaldehyde and 0.1% glutaraldehyde in PBS overnight at 4 °C. Dehydration was carried out with a series of ethanol washes. Samples were embedded in LR White resin (OKEN) according to the manufacturer's protocol. Thin sections were cut with diamond knives and mounted on nickel grids. The sections were blocked with 3% BSA in PBS for 30 min. Sections were then incubated with anti-GFP antibody (1:30 v/v) in PBS containing 1% BSA overnight at 4 °C, followed by incubation with 10-nm gold-particle-conjugated secondary antibody (1:30 v/v) for 1 h at room temperature. Samples on grids were counter stained with 2% (wt/vol) uranyl acetate and then observed with a JEM-1220 electron microscope (JEOL). Image J was used to quantify the gold particles and the area of phagosomes.

Isolation of microbead and M.tb phagosomes. Six 15-cm plates of Raw264.7 cells were used for each condition. For isolation of the microbead phagosomal fraction, microbeads (2 μm, Polyscience) were added to Raw264.7 cells for 1 h, washed three times with prewarmed DMEM and incubated in DMEM with 10% FBS for the indicated times. Raw264.7 cells were then collected, lysed, and subjected to discontinuous sucrose gradient centrifugation as described previously [4]. For isolation of the *M.tb* phagosomal fraction, bacteria at an MOI of 10–30 were added to Raw264.7 cells in DMEM with 10% FBS for 1 h, washed and then incubated for the indicated times. Infected cells were collected, lysed, and subjected to fractionation as described previously [15]. For immunoblotting analysis, aliquots of 12.5 μg of Raw264.7 cell lysate and 3 μg of phagosomal fraction proteins were separated by SDS–polyacrylamide gel electrophoresis (PAGE) and then subjected to immunoblotting analysis using anti-Rab7 antibody (1:200 v/v), anti-LAMP-2 antibody (1:200 v/v), anti-cathepsin D antibody (1:200), and anti-cytochrome C (1:100 v/v). Band intensities from three independent experiments were quantified by Image J (http://rsb.info.nih.gov/ij/).

Immunofluorescence microscopy. Raw264.7 cells grown on round coverslips in 12-well plates were allowed to phagocytose microbeads or infected with bacteria for the indicated times, fixed with 3% paraformaldehyde in PBS for 1 h at room temperature, permeabilized with 0.1% Triton X-100 in PBS for 5 min, and finally washed with PBS. Fixed cells were blocked with 3% bovine serum albumin in PBS for 1 h followed by staining with the anti-LAMP-2 (1:50 v/v), cathepsin D (1:50 v/v) antibodies for 1 h, and then incubated with Alexa488- or Alexa546-conjugated anti-IgG antibodies (1:1000 v/v) for 1 h.

Statistics. The unpaired two-sided Student's *t*-test was used to assess the statistical significance of differences between the two groups.

Results and discussion

Rab7 transiently localizes on M.tb phagosome

Rab7 has been shown to be absent from mycobacterial phagosomes in macrophages at the time point when its recruitment generally occurs [9,10]. On the other hand, Clemens and Horwitz demonstrated that *M.tb* phagosomes acquired Rab7 in infected HeLa cells [16], and Sun et al. demonstrated the presence of Rab7 on *Mycobacterium bovis* Bacilus Calmette-Guérin phagosomes [17]. However, there are no crucial reports about the interaction between Rab7 and *M.tb* phagosomes in infected macrophages, especially the kinetics of Rab7 localization immediately after infection. We first examined the localization kinetics of Rab7 on the phagosomes in *M.tb*-infected macrophages. For this purpose, Raw264.7 macrophage cell line expressing enhanced GFP fused with Rab7 (EGFP-Rab7) was employed, because no satisfactory staining was obtained with the commercially available anti-Rab7 antibodies. Raw264.7 cells expressing EGFP-Rab7 were infected with *M.tb* expressing DsRed for 30 min or 6 h. Rab7 failed to localize on the majority of *M.tb* phagosomes at 6 h postinfection (Fig. 1B), although clear signals of EGFP-Rab7 was observed on the phagosomes at 30 min postinfection (Fig. 1A). The proportion of Rab7-positive phagosomes containing *M.tb* reached approximately 80% at 30 min postinfection, as observed in macrophages infected with *S. aureus*, and it decreased to about 30% by 6 h (Fig. 1C) and remained at this level until at least 12 h (data not shown). That of *S. aureus* retained more than 80% at 6 and 12 h postinfection (Fig. 1C and data not shown). Rab7 localized on about 75% of heat-inactivated *M.tb* phagosomes at 6 h after phagocytosis (Fig. 1D), suggesting that live *M.tb* actively promotes Rab7 dissociation from the phagosome.

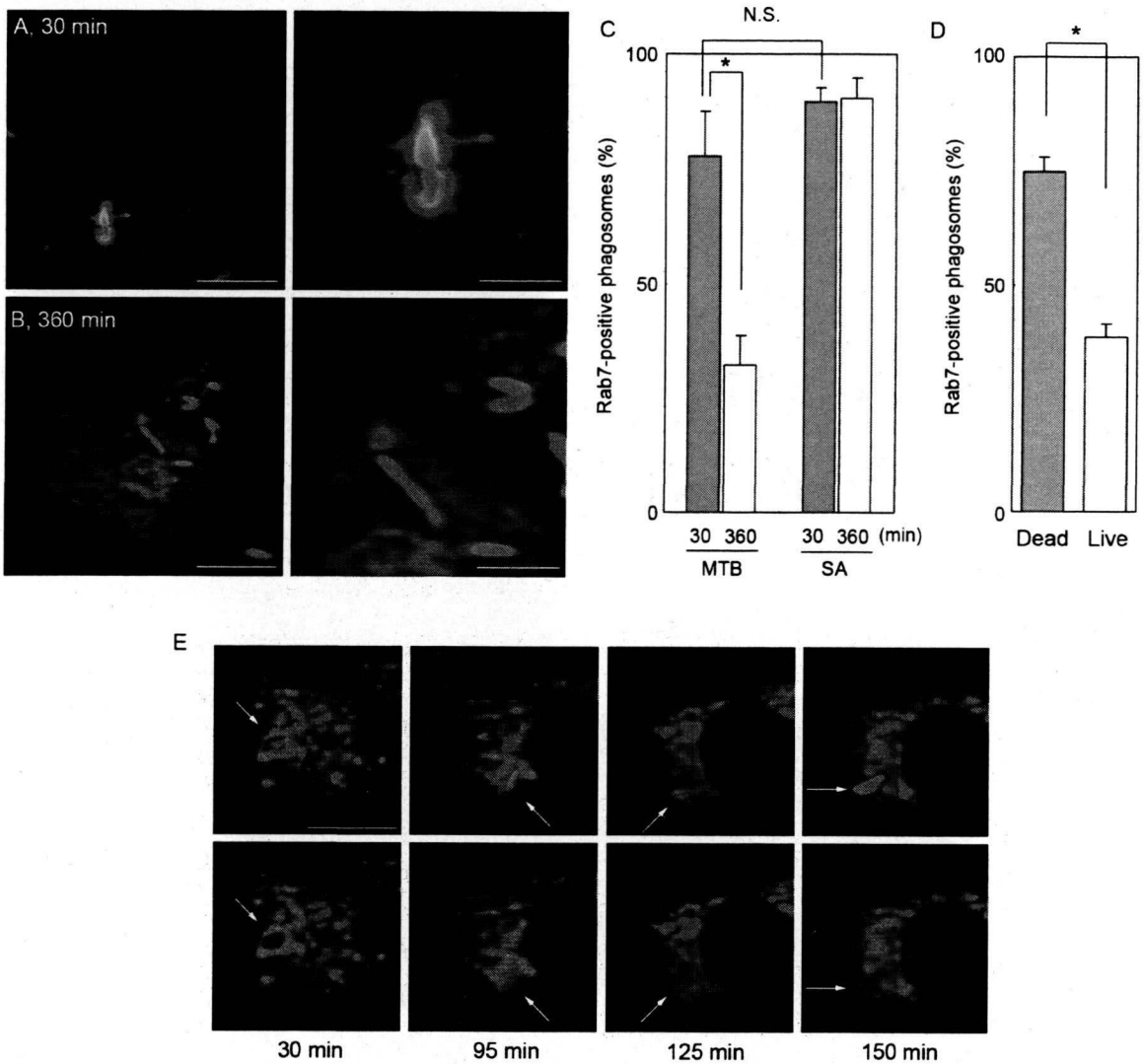

Fig. 1. Dynamics of Rab7 localization on *M.tb* phagosomes. (A, B) Raw264.7 cells expressing EGFP-Rab7 were infected with *M.tb* (MTB) expressing DsRed for 30 min (A) or 6 h (B). Cells were then fixed and observed with confocal microscopy. The right panels show the enlarged images of the phagosomes shown at left. Scale bar, 10 μm (left panel), 3 μm (right panel). (C) The proportion of Rab7-positive phagosomes containing *M.tb* (MTB) and *S. aureus* (SA) at 30 min and 6 h postinfection. (D) The proportion of Rab7-positive phagosomes containing live (Live) and heat-inactived (Dead) *M.tb* at 6 h postinfection. Data represent the average of three independent experiments in which more than 200 phagosomes were counted for each condition in (C) and (D). $^{*}P < 0.05$. N.S., no significance. (E) Raw264.7 cells expressing EGFP-Rab7 were infected with *M.tb* expressing DsRed and analyzed by 4D microscopy. The upper and lower panels show fluorescent images of the same Raw264.7 cell expressing EGFP-Rab7 (green) with or without fluorescent images of *M.tb* (red), respectively, at the indicated times after infection. Arrow indicates *M.tb* phagosome. Scale bar, 10 μm.

We investigated the dynamics of EGFP-Rab7 localization on *M.tb* phagosomes by live 4D confocal microscopy (Fig. 1E and Movie S1). At 30 min postinfection, Rab7 was clearly present on the *M.tb* phagosome. The outline of the Rab7 signal surrounding the phagosome began to fade at 95 min and disappeared completely at 125 min. At 150 min postinfection, Rab7 was still absent from the phagosome. These results suggest that Rab7 started to localize on the majority of *M.tb* phagosome immediately after infection, but viable *M.tb* subsequently caused the dissociation of Rab7 from the phagosome.

We applied immunoelectron microscopy to investigate Rab7 localization on *M.tb* phagosomes. Macrophages expressing EGFP-Rab7 were infected with *M.tb* for 30 min or 6 h, fixed and processed for immunoelectron microscopy using anti-GFP antibody. Gold particles forming clusters were associated with *M.tb* phagosome membranes at 30 min, but not at 6 h postinfection (Fig. 2A and B). Quantitative analysis revealed that about 80% of *M.tb* phagosomes is associated with gold particles forming clusters at 30 min and that the number of gold particles associated with *M.tb* phagosomes was remarkably decreased at 6 h (Fig. 2C). These results suggest that *M.tb* phagosomes acquire Rab7 molecules by the association with Rab7-containing vesicles immediately after infection, and that this association is canceled at the later stage of infection.

To confirm biochemically that Rab7 is transiently recruited to and then dissociated from *M.tb* phagosomes, we conducted immunoblotting analysis to detect Rab7 in isolated mycobacterial phagosomal fractions. Raw264.7 macrophages were allowed to phagocytose microbeads or infected with *M.tb* for 30 min or 6 h, and the phagosomal fractions were isolated as previously reported [4,15]. We checked the purity of phagosomes by thin-section electron microscopy and immunoblotting analysis for cytochrome C, and found that few organelles and materials had contaminated in both phagosomal fractions (Supplemental Fig. 1). As shown in Fig. 3, the amount of Rab7 on *M.tb* phagosomes at 6 h postinfection decreased significantly to 19 ± 7% (mean ± standard deviation,

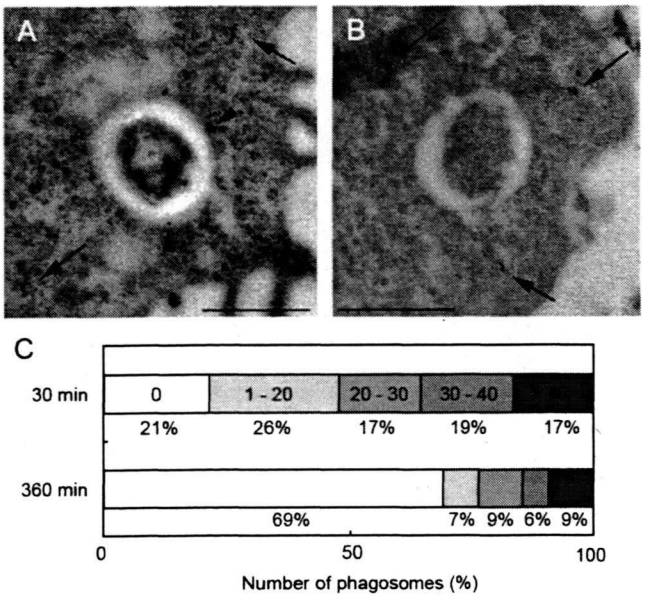

Fig. 2. Immunoelectron microscopic analysis of Rab7 localization on *M.tb* phagosomes. (A, B) Immunoelectron microscopic images of *M.tb*-infected macrophages. Raw264.7 macrophages expressing EGFP-Rab7 were infected with *M.tb* for 30 min (A) or 6 h (B) and processed for immunoelectron microscopy. Thin sections were stained with anti-GFP antibody followed by 10-nm gold-particle-conjugated secondary antibody. Arrow and arrowhead indicate gold particles forming clusters in the cytoplasmic region and on the phagosome, respectively. Scale bar, 0.5 μm. (C) Distribution of Rab7-gold particles associated with *M.tb* phagosomes. The number of gold particles on each *M.tb* phagosome in EGFP-Rab7-positive macrophages was counted at 30 min ($n = 52$ phagosomes) or 6 h ($n = 56$ phagosomes) postinfection, and the number per area (μm^2) of each phagosome was calculated. The distribution of the number of gold particles associated with the phagosome is indicated in the bar. The percentages of the different populations are shown at each time point.

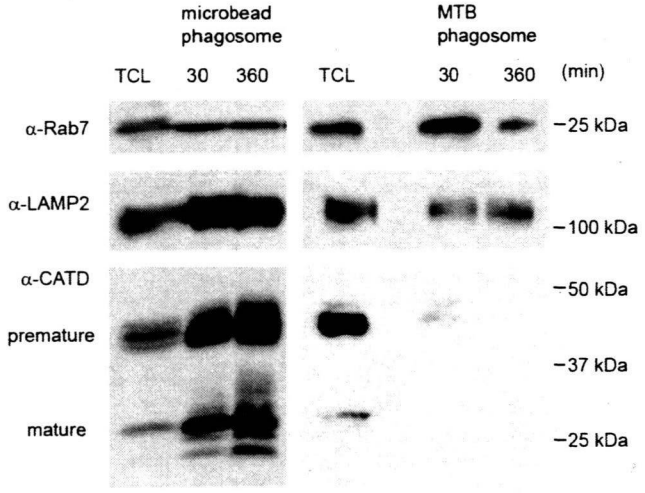

Fig. 3. Rab7 localization in isolated *M.tb* phagosomal fractions. Immunoblotting analysis of microbead and *M.tb* (MTB) phagosomal fractions with antibodies to Rab7, LAMP-2, and cathepsin D (CATD) is shown. Total cell lysates from Raw264.7 cells (TCL) and phagosomal fractions of microbead or *M.tb* were subjected to SDS-PAGE, followed by immunoblotting using indicated antibodies.

$n = 3$, $P < 0.05$) of that at 30 min, whereas the amounts on microbead phagosomes at 30 min and 6 h were nearly the same. These results are in line with those obtained by immunofluorescence and immunoelectron microscopic analyses and support the idea that Rab7 is transiently recruited to and then dissociated from *M.tb* phagosomes.

Localization of the constitutively active form of Rab7 on M.tb phagosome

It seems most likely that the dissociation of Rab7 from *M.tb* phagosomes is caused by *M.tb*-mediated conversion of its form from the GTP-bound type to the GDP-bound one. To investigate the mechanism by which Rab7 is released from *M.tb* phagosomes after transient recruitment, we employed the constitutive-active Rab7 mutant Rab7Q67L which lacks GTPase activity [18]. EGFP-fused Rab7Q67L localized on the majority of *M.tb* phagosomes at 30 min postinfection, and were dissociated from phagosomes at 6 h (data not shown), just as for the wild type of Rab7 (Fig. 1). These results suggest that the GTPase activity of Rab7 is not required for the dissociation of Rab7 from *M.tb* phagosomes. We propose two possibilities to account for the GTPase-independent dissociation of Rab7 from *M.tb* phagosomes. First, Rab7 dissociation is caused by the inactivation of the tethering and/or docking molecules of Rab7 to *M.tb* phagosome, which leads to the increase of Rab7 efflux from the phagosome. Second, vesicles containing Rab7 are transiently associated with and then dissociated from *M.tb* phagosomes at the early and late stages of infection, respectively, as shown by immunoelectron microscopy (Fig. 2).

Localization of lysosomal proteins on M.tb phagosome

To further understand the effect of Rab7 dissociation from the phagosome, we examined that lysosomal marker proteins depend on the function of Rab7 to localize on the phagosome (Fig. 4). We chose LAMP-2 and cathepsin D that have been shown to reside on microbead phagosome [19] as the lysosomal markers. Raw264.7 macrophages simultaneously transfected with two plasmids encoding EGFP and a dominant-negative form of Rab7, Rab7T22N, were allowed to phagocytose microbeads for 2 h and then stained with anti-LAMP-2 or anti-cathepsin D antibodies. In the wild type Raw264.7 cells, both lysosomal markers are localized on more than 80% of microbead phagosomes at 2 h after phagocytosis (data not shown). In Raw264.7 cells expressing Rab7T22N, LAMP-2 was recruited to microbead phagosomes (Fig. 4A), while cathepsin D was not (Fig. 4B). The results indicate that LAMP-2 on the phagosome is Rab7-independent, while that of cathepsin D is Rab7-dependent.

Both LAMP-2 and cathepsin D showed limited localizations on mycobacterial phagosomes in macrophages 24 h after infection and later [6]. However, the kinetics of their localization on mycobacterial phagosomes immediately after infection is not known. We therefore examined the localization of LAMP-2 and cathepsin D on *M.tb* phagosomes by immunofluorescence microscopy (Fig. 4). LAMP-2 localized on about 80% and 60% of *M.tb* phagosomes at 30 min and 6 h postinfection, respectively (Fig. 4C and D). Cathepsin D localized on about 50% of phagosomes at 30 min postinfection, but its localization on *M.tb* phagosome showed a punctuated staining pattern (Fig. 4E). At 6 h postinfection, it was not present on most *M.tb* phagosomes (Fig. 4F).

Localization of LAMP-2 and cathepsin D on isolated *M.tb* phagosomes was examined by immunoblotting analysis (Fig. 3C). Both lysosomal markers were present in the microbead phagosomal fractions, as previously reported [19]. In the *M.tb* phagosomal fractions, LAMP-2 was present, but cathepsin D was absent at 30 min and 6 h postinfection. The results obtained by immunofluorescence microscopic and immunoblotting analyses suggest that LAMP-2 localizes on the major proportion of *M.tb* phagosomes and that cathepsin D associates with *M.tb* phagosome immediately after infection, but the fusion of cathepsin D with *M.tb* phagosome is inhibited.

In conclusion, we propose the following model for *M.tb*-induced inhibition of phagolysosome biogenesis based on the data pre-